7.08 The Dynamics and Convective Evolution of the Upper Mantle

EM Parmentier, Brown University, Providence, RI, USA

7.08.1 Introduction

The thermal structure of the oceanic upper mantle plays an important role in the larger-scale dynamics of the mantle. Fortunately, this region of the Earth is one that is accessible to observation by a variety of geophysical tools and so can provide a basis for understanding solid-state convective instability, with implications for even more general settings than the Earth's upper mantle. It can be argued that the Earth's upper mantle is the best natural laboratory available to us to study the convective evolution of planetary interiors.

The goal of this chapter is to summarize current understanding of the evolution of the upper mantle based on observations and theoretical predictions, beginning with some of the earliest observations on how cooling the mantle from above would be expressed in seafloor depth, heat flow, and geoid height as functions of age. It is not possible to consider the role of convective instability in the upper mantle in isolation from other forms of larger-scale mantle flow. While no general agreement has yet emerged on how various scales of convection may affect the upper mantle, small-scale thermal convective instability generated within the upper mantle provides a viable explanation for many important observations. Convection in the upper mantle may be driven by buoyancy resulting both from cooling at the surface and by melting. Mantle cooling is expressed in oceanic heat flow and in geoid height and seafloor depth through the effect of cooling on mantle density.

Buoyancy due to melting may be expressed in intraplate volcanism. Only a few long-lived, age-progressive, linear volcanic chains meet all the criteria of the deep mantle plume-fixed hot spot hypothesis (see 00010, this volume). Decompression melting in small-scale thermally driven convective upwellings has been one favored explanation for volcanic ridges aligned with plate motion. Seafloor volcanism may also reflect spontaneously generated instability driven by decompression melting, which has been termed 'magmatic convective storms.' Buoyant decompression melting beneath moving plates is one possible mechanism for the abundant short-lived island chains and volcanic ridges identified on the Earth's seafloor.

Finally, the role of mantle upwelling and melting beneath spreading centers is important to consider, in part because it is responsible for the generation of the oceanic crust and is a factor controlling spreading center structure. However, melting and melt extraction under spreading centers leave behind residual mantle that is transported away from the spreading center. Compositional changes are expected to affect viscosity or creep rate and create a stable chemical stratification, thus fundamentally influencing convective instability everywhere in the upper mantle (Kohlstedt, Vol. 2).

7.08.2 Cooling the Mantle from Above

7.08.2.1 An Historical Perspective

Turcotte and Oxburgh (1967) identified the moving lithospheric plates (Wessel, Vol. 6) as the conductive thermal boundary layer at the top of mantle convection cells, thus

 http://dx.doi.org/10.1016/B978-0-444-53802-4.00131-7

establishing a physical relationship between upper mantle thermal structure and mantle dynamics. During the emergence of plate tectonics, measurements of seafloor depth and heat flow in the oceans provided the first direct evidence on the thermal structure of the upper mantle. Heat flow generally decreased with crustal age but showed great variability, particularly at young ages. This variability is now understood to be due primarily to hydrothermal circulation of seawater through permeable crustal rocks. In contrast, seafloor depths showed a much more systemic variation with seafloor age. The age dependence of isostatic seafloor depth, which depends on the depth-averaged temperature, was recognized as a stronger observational constraint than heat flow on upper mantle thermal structure (Langseth et al., 1966; McKenzie, 1967; McKenzie and Sclater, 1969; Sleep, 1969; Vogt and Ostenso, 1967).

The thermal structure that develops due to conductive cooling should be, at least to first order, only a function of crustal age, rather than an independent function of both distance from spreading center and plate velocity. Observations of seafloor depth and age generally confirmed this age dependence. The Turcotte and Oxburgh boundary layer hypothesis, in the simple form suggested originally, indicated that the thermal boundary layer should continue to thicken as the square root of age so that old seafloor would continue to subside. This did not appear to explain observations showing a relatively uniform depth of old seafloor that required that the thermal boundary layer evolve to a nearly constant thickness. Models for upper mantle thermal structure that were consistent with average depth of seafloor as a function of age from the growing collection of observations treated the conductive cooling of horizontally moving upper mantle, as in the simple boundary layer theory, but with the added assumption of a uniform temperature at a prescribed depth (Langseth et al., 1966; McKenzie, 1967). A relatively uniform seafloor depth at old ages requires a mechanism to transport heat to the bottom of the thermal boundary layer, thus reducing the rate at which it thickens. This set the stage for research in the following several decades and is still a source of continuing study and debate.

7.08.2.2 Convective Instability Versus Heating by Hot Spots: Depth–Age and Heat Flow

Both small-scale convective instability of the cool thermal boundary and heating at hot spots (McNutt, Vol. 1; 00009, this volume) may play a role in transporting heat to the bottom of the thermal boundary layer, but no general consensus has yet emerged on a single mechanism of heating that can explain all available observations. Ideally, observed variations in seafloor depth might constrain the relative importance of these two mechanisms, but such interpretations are limited by the relatively small amount of old seafloor with a well-determined age, by the uncertainty in correcting for the thickness and load of sediments, and by unidentified crustal thickness variations. Many earlier studies have shown that simply averaging all depth measurements at a given age indicates that old seafloor is, on average, shallower than would be predicted by conductive cooling alone. Several recent studies have continued to refine earlier interpretations of a seafloor depth–age relationship (Crosby and McKenzie, 2009; Crosby et al., 2006; Hillier and Watts, 2005). As shown in **Figure 1** and as further discussed in the succeeding text, differing methodology in these

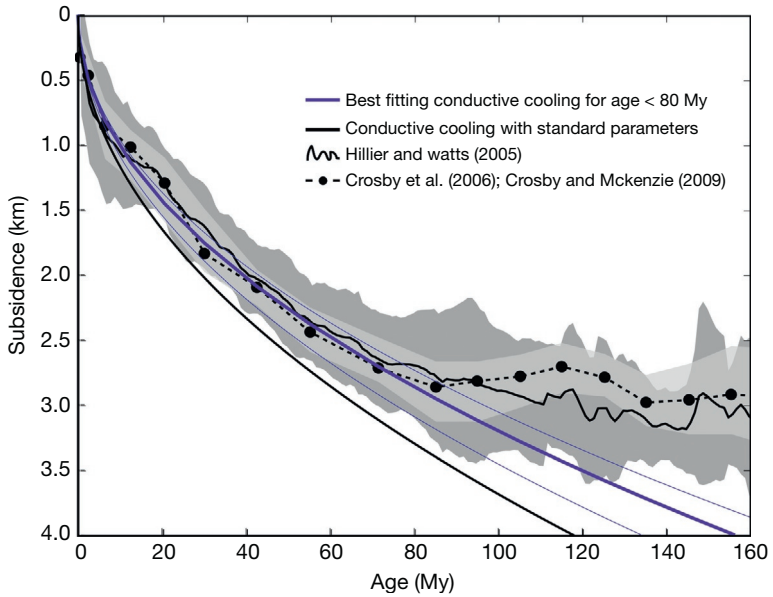

Figure 1 Estimates of seafloor depth as a function of age for various oceans, based on depths corrected for sediment and crustal thickness variations, compared to conductive cooling models. The black curve is from Hillier and Watts (2005) with the darker shaded region showing one standard deviation about the mean value at each age. The black dashed curve is from Crosby et al. with the light shaded region showing the variation in topography observed in a given age bin. Different criteria used to define 'normal' seafloor, discussed in the text, account differences shown. The solid black line corresponds to conductive cooling with nominal values of thermal diffusivity (10^{-6} m^2 s^{-1}), thermal expansivity (3×10^{-6} K^{-1}), mantle density (3300 kg m^{-3}), and mantle temperature (1350 °C) giving a subsidence rate of 386 m Ma$^{-1/2}$. The blue curves correspond to a best-fitting subsidence rate (325 ± 20 m Ma$^{-1/2}$) for seafloor younger than 70 My.

studies leads to different depth–age estimates. However, in both studies, old seafloor appears to be at least several hundred meters shallower than the depth predicted by a purely conductive cooling model that fits well at ages <70 My. So the long-standing question is: why is old seafloor often shallower than predicted by conductive cooling alone, and how is it possible to infer the physical process(es) responsible?

Heating due to hot spots should correlate with the length of time that a given area of seafloor has spent in the proximity of a hot spot (Crough, 1975). Heestand and Crough (1981) sorted the depth of seafloor in the North Atlantic by distance from the nearest hot spot track. Comparing depth–age for seafloor in constant distance ranges indicated no flattening at old ages. Hayes (1988) noted that in the South Atlantic, where hot spot influences appear to be less significant, depth followed a purely conductive cooling curve to ages approaching 120 My but noted the complication of a persistent asymmetry in apparent subsidence rate across the spreading axis. An asymmetry in the apparent subsidence rate was also found in the southeast Indian Ocean (Hayes, 1988) and across the East Pacific Rise (Eberle and Forsyth, 1995). One possibility may be that this asymmetry reflects the dynamic topography of larger-scale mantle flow on which the depth–age subsidence is superimposed (Jian Lin, Vol. 6).

The Pacific Plate contains not only relatively large areas of old seafloor but also numerous seamounts and hot spot tracks (e.g., Wessel and Lyons, 1997). Studies like those cited in **Figure 1** have compiled seafloor depth–age curves for the Pacific and other ocean basins, often with differing results depending on the criteria used to exclude seafloor affected by volcanism or other processes. Schroeder (1984) found that eliminating data within 800 km of hot spot tracks resulted in a good correlation of depth with square root of age for ages <80 My. All seafloor older than 80 My was shallower than predicted by conductive cooling alone but was within 800 km of hot spots or hot spot tracks. Renkin and Sclater (1988) analyzed the effect of uncertainties in basement age and sediment thickness on depth–age correlations in the North Pacific. Arguing that volcanic constructs always result in shallower seafloor, they proposed that modal seafloor depth, or more precisely a range enclosing 2/3 of the measured depths at any age, provides an estimate of subsidence associated with cooling least biased by volcanism. Modal depths increase with age more slowly than predicted by conductive cooling for ages exceeding about 80 My. Plotting modal depths with age along a corridor of the Pacific seafloor containing several swell-like features, Renkin and Sclater argued that not even the deepest depths fall along a conductive cooling model. The studies of Hillier and Watts (2005) and Crosby et al. (2005) shown in **Figure 1** are among the more recent studies illustrating that differing criteria for identifying normal seafloor (not affected by processes other than simple aging) lead to different estimates of a depth–age relationship. Hillier and Watts (2005) employed a filtering technique that appears to be an automation of visual inspection. After excluding by eye seafloor thought to be affected by hot spot chains and oceanic plateaux, Crosby et al. used the absence of gravity anomalies to identify seafloor included in their depth–age compilation seafloor. Korenaga and Korenaga (2008) used both distance from hot spot chains and statistical correlation criteria. Both Crosby et al. (2005) and Korenaga and Korenaga (2008) found best-fitting square root of age subsidence rate that is smaller than predictions based on mineral physics data. Korenaga and Korenaga (2008) attributed this to a lower effective thermal expansivity of a viscoelastic mantle (Korenaga, 2007). An interesting conclusion of both Crosby et al. (2005) and Korenaga and Korenaga (2008) is a strong correlation between zero-age depth and subsidence rate. The possible cause or implications of this correlation have not yet been addressed.

Small-scale convective instability of the thermal boundary layer, in addition to hot spots, may advectively transport heat to the bottom of the conductive boundary layer. The possible importance of small-scale convection was first suggested on the basis of averaged depth–age curves that deviate from purely conductive cooling at a seafloor age of about 70–80 My, which was presumed to correspond to the onset of convective instability (Parsons and McKenzie, 1978). Beyond this age, convective heat transfer was thought to maintain the nearly constant thermal boundary layer thickness implied by the plate model (Davis and Lister, 1974; Parsons and Sclater, 1977; Stein and Stein, 1992). Plate thickness must be consistent with the heat flow measured on old seafloor (Davis et al., 1984; Lister et al., 1990; Nagihara et al., 1996) and its depth. **Figure 2** from Nagihara et al. (1996) shows heat flow values for old seafloor in the northwestern Pacific and in the western North Atlantic, both areas where high-quality heat flow and data needed to correct depth for sediment loading and crustal thickness variations are available. Also shown are predictions from two versions of the plate model and purely conductive cooling, all of which are thought to provide reasonable fits to the depth–age relationship of younger seafloor. Heat flow is higher and seafloor is consistently shallower than predicted by conductive cooling. The plate model of parameters of Parsons and Sclater (1977) with a plate thickness 125 km and a mantle temperature 1350 °C fits the depths well but underestimates the heat flow. In contrast, the hotter and thinner plate model of Stein and Stein (1992) with a plate thickness 95 km and a mantle temperature 1450 °C fits the heat flow well but underestimates old seafloor depth. It is worth noting that this mantle temperature is significantly higher than that estimated from melting in adiabatically upwelling mantle beneath spreading centers, frequently inferred to be 1325–1350 °C. In contrast to thermal evolutions with a constant temperature at a prescribed depth, constant heat flux from below (Doin and Fleitout, 1996) also appears to fit the observations within some appropriately defined uncertainties. Goutorbe and Hillier (2013) provided a recent comparison of the fit of these two models to observations.

Thus, numerous studies have found that seafloor older than 70–90 My reaches depths several hundred meters shallower than would be predicted by simple conductive cooling of the upper mantle; and this has typically been explained by some form of heat transfer from the deeper mantle. The usual assumption of a constant crustal thickness implies melting due to upwelling of mantle beneath spreading centers with a time-independent potential temperature and composition. For plausible ranges of crustal and mantle densities, only an additional 400 m of crust would be required to elevate the seafloor by 100 m. Given the small number of accurate measurements of crustal thickness in old oceanic areas particularly the large

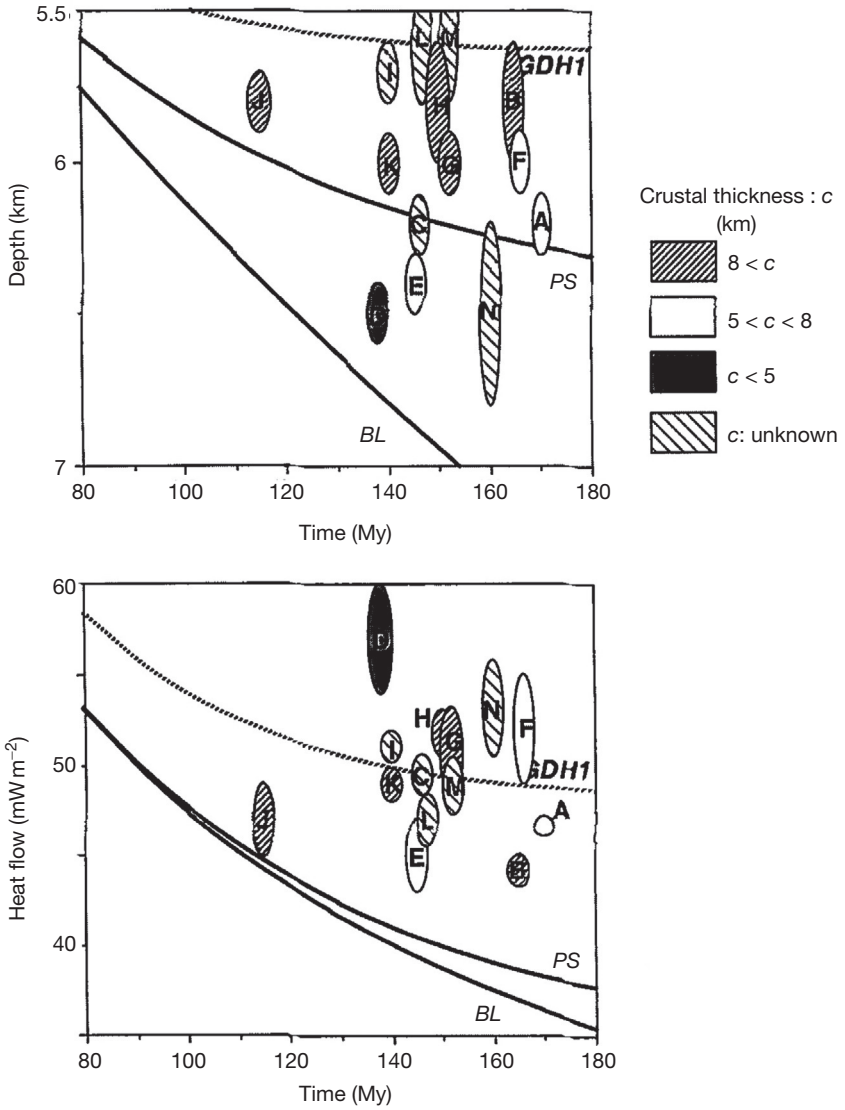

Figure 2 Seafloor basement depth (top), corrected for sediment load and crustal thickness where available, and heat flow (bottom) at sites in the western North Pacific (A–X) and northwestern Atlantic (X–Z) as functions of age from Nagihara et al. (1996). The location of specific sites is identified in the Table 1 and Figure 1 of Nagihara et al. Model curves for the plate models (PS and GDH1) and half-space cooling (BL).

areas of old seafloor in the western Pacific (Oikawa et al., 2010; White et al., 1992), the possibility of a secular increase in crustal thickness and associated depleted mantle lithosphere due to a change in potential temperature or composition of the upper mantle might deserve more consideration. The large number of volcanic seamounts in parts of the Pacific Plate older than 80 Ma has been long recognized and was recently discussed by Hillier (2006). Conrad et al. (2011) attributed this to a time of rapid plate motion and mantle shearing. Alternatively, this has been attributed to a global-scale change in upper mantle thermal structure (Larson, 1991) that could explain a range of geologic observations (Larson and Erba, 1999). Additional attention to measures of upper mantle thermal and compositional structure in addition to depth–age will be required to distinguish between various explanations of seafloor depth evolution.

7.08.2.3 Geoid Height as a Measure of Upper Mantle Thermal Structure

As discussed previously, the earliest interpretations of the thermal evolution of the upper mantle relied largely on heat flow and isostatic seafloor depth, with the isostatic assumption justified by the absence of free-air gravity anomalies correlated with the depth–age variation. Following the advent of sea surface elevation measurements from satellite altimetry, the long-wavelength geoid (Jekeli, Vol. 3) and gravity provided further constraint on upper mantle thermal structure (Chase, 1985; Smith, 1998). Isostatic seafloor depth measures the density averaged over depth in the mantle; geoid height measures the first moment of the density distribution with depth (Haxby and Turcotte, 1978). Conductive cooling predicts that geoid height decreases linearly with age

(Haxby and Turcotte, 1978) as they observed along a GEOS-3 altimetry track in the North Atlantic. Also, using early GEOS-3 altimetry data, Sandwell and Schubert (1980) found that geoid height decreases approximately linearly with seafloor age for ages less than about 80 My in the Atlantic and southeast Indian spreading centers with geoid slopes in the range −0.131 to −0.149 m My^{-1}, generally consistent with a conductive cooling thermal boundary layer. In contrast, the geoid height predicted by the plate model should flatten over old seafloor. Sandwell and Schubert (1980) found that geoid height in the southeast Pacific was not consistent with a simple linear geoid–age relationship but decreased rapidly with age. The decrease was much more rapid than predicted by the plate model used to explain flattening of old seafloor. This is further discussed in the succeeding text.

The geoid height is sensitive to density variations over much larger spatial scales than gravity anomalies. Therefore, density variations throughout the Earth, not just in the upper mantle, contribute to geoid height variations. The difficulty in using geoid as a constraint on the age dependence of the upper mantle is to separate variations in geoid height with seafloor age from other contributions, for example, from oceanic swells or hot spots. One approach to filtering out the long-wavelength contributions is to measure the change in geoid height across fracture zones that juxtapose seafloor of different ages (Crough, 1979a; Detrick, 1981). If geoid height decreases linearly with age as expected for conductive cooling, the change in geoid height across a fracture zone of constant age offset should remain constant as seafloor on each side of the fracture zone ages. In contrast, the plate model should show a change in geoid height across the fracture zone that decreases with age and that vanishes once thermal boundary layer thickness becomes constant. Observations suggest that geoid slope decreases with age, but it appears to do so at a much earlier age than that at which the seafloor flattens. Studies of variations of geoid height with age include Cazenave (1984), Driscoll and Parsons (1988), and Freedman and Parsons (1990). Geoid height as a function of age from Cazenave (1984), plotted as geoid–age slope, is shown in **Figure 3**.

Determining the geoid height change with age using measurements across fracture zones is elegant in concept but difficult in practice. Mechanical behaviors of lithosphere, both plate flexure associated with differential subsidence (Sandwell and Schubert, 1982a,b) and thermal bending (Parmentier and Haxby, 1986; Wessel and Haxby, 1990), create uncompensated seafloor topography over distances of 50–100 km adjacent to fracture zones. The resulting geoid anomalies may obscure the identification of the change in isostatic geoid height. Despite these uncertainties, geoid height variation with age is not explained by either the half-space cooling or the plate model mantle thermal structure.

7.08.2.3.1 Intraplate seismicity and plate elasticity as an indicator of thermal structure

The age dependence of the apparent elastic thickness of the oceanic lithosphere can also constrain the variation of mantle thermal structure with age. Focal depths of oceanic intraplate earthquakes increase with age following a 650–700 °C isotherm in a conductive cooling model (Bergman and Solomon, 1984; Weins and Stein, 1984). However, most of the seismicity reported occurs at ages <70 My and so does not constrain thermal structure at older ages. Flexure of lithosphere at trenches should also reflect the mechanical thickness. Levitt and Sandwell (1995) indicated that plate thickness increases with age of subducting lithosphere and that the plate in the Stein and Stein (1992) thermal model may be too hot and thin. But the data do not resolve the difference between a simple conductive cooling and a plate model with a thicker plate.

7.08.2.4 Seismic Velocity and Attenuation as Measures of Upper Mantle Structure and Flow

Seismic velocities and attenuation in the upper mantle (Montagner, Vol. 1 and (Rainer) Kind, Vol. 1) also constrain thermal structure and its age evolution. Surface wave dispersion has been used to infer the velocity variation with age and depth (Maggi et al., 2006a,b,c; Nettles, 2006; Nettles and Dziewonski, 2008; Nishimura and Forysth, 1989; Priestly and McKenzie, 2006; Ritzwoller et al., 2004; Weeraratne et al., 2007; Zhou et al., 2006). As shown in **Figure 4**, seismic shear wave velocities generally decrease with depth at a given age and increase with age at a given depth. Seismic velocities, which increase with decreasing temperature, continue to change with age at depths exceeding 150 km. Using the parameterizations of Priestley and McKenzie (2006) as a first attempt to assess the

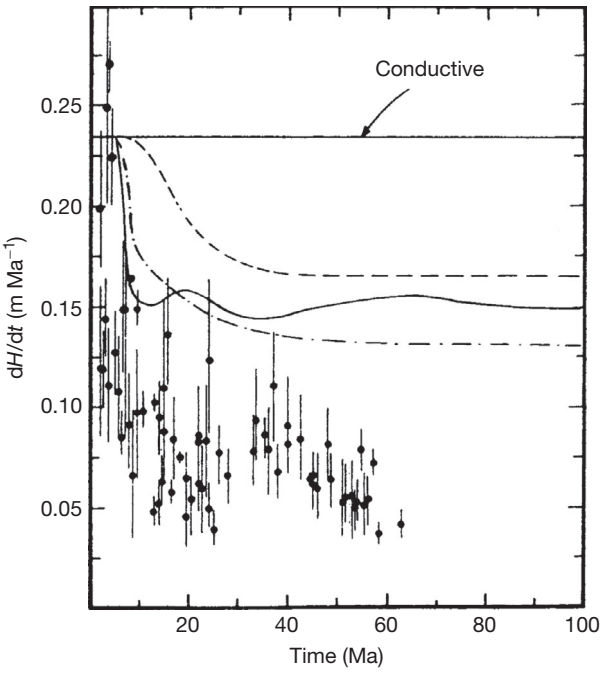

Figure 3 Geoid–age slope as a function of age with data from Cazenave (1984). Pure conductive cooling leads to the constant geoid–age slope as shown. The observations indicate a rapid decline with age. Curves show model predictions from Buck and Parmentier (1986) for convective cooling with an activation energy of 420 kJ mol^{-1} and an activation volume of 10 cm^3 mol^{-1}. Dashed and long–short dashed curves are for a model reference viscosity of 10^{18} Pa s and 5×10^{18} Pa s, respectively. The solid curve is also for a 10^{18} Pa s viscosity but in a wider and more finely discretized model domain.

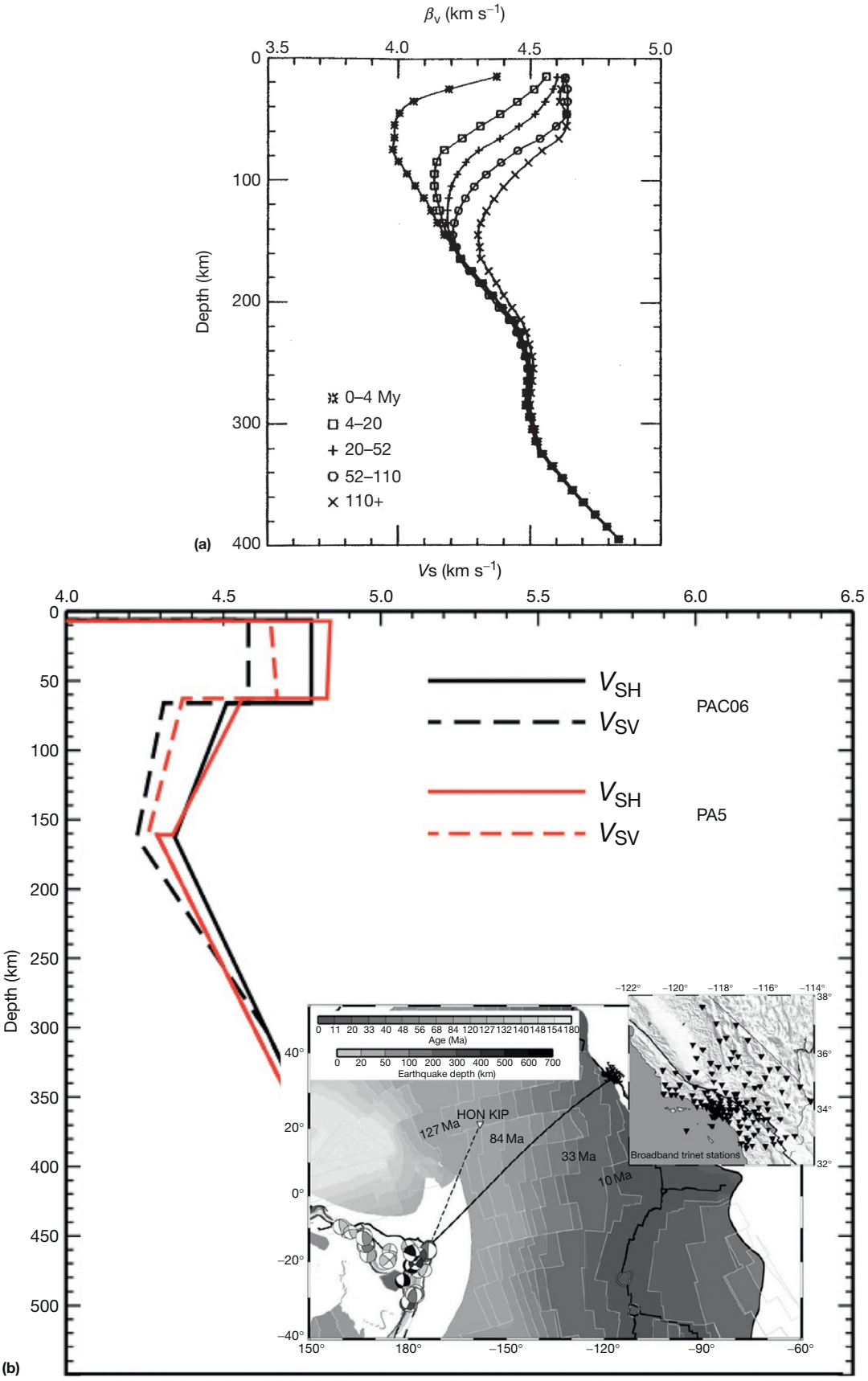

Figure 4 (a) Vertically polarized shear wave velocity in the Pacific as a function of depth in various age intervals determined from Rayleigh wave dispersion (Nishimura and Forsyth, 1989). Note that shear wave velocity changes with age at depths greater than would be consistent with a plate model that fits the depth–age relationship ($\leq$125 km). Changes with age continue beneath seafloor with ages exceeding 110 My. (b) Shear wave velocity as a function of depth derived from *S*-wave reverberations along paths in the Pacific Plate modified from Tan and Helmberger (2007). Velocity is shown for both horizontally (SH) and vertically (SV) polarized shear waves. PA5 is for the corridor from Tonga–Fiji to Hawaii (Gaherty et al., 1996) and PAC06 is for the corridor from Tonga–Fiji to the TriNet array in Southern California (Tan and Helmberger, 2007).

role of temperature alone on seismic velocity, the velocity change of 0.1 km s^{-1} at 150 km depth between 52 and 110 My and >110 My would require cooling in the range of 100–200 °C. Unless some mechanism other than cooling causes the velocity increase, this clearly contradicts the plate model that implicitly assumes that mantle temperature at depths greater than the plate thickness does not change with age. Seismic velocity distributions like those in **Figure 4** may also constrain the depth to which convective instability has cooled or in some other way affected the mantle. Early studies like that of Nishimura and Forsyth (1989) probably do not resolve variations deeper than ~200 km. More recent studies using longer-period (and consequently longer-wavelength) surface waves (Maggi et al., 2006a,b,c; Nettles and Dziewonski, 2008; Zhou et al., 2006), which should resolve velocity variations to greater depth, indicate variations deeper than 200 km. However, the extent to which these variations correlate with plate age has not been established.

Surface waves, because of their long wavelength, have limited depth resolution in sampling mantle velocities. High-frequency body waves are required to detect short-wavelength variations in seismic velocity. Since the pressure, or depth, of phase changes in the upper mantle (Oganov, Vol. 2) depends on temperature, temperature variations should be reflected in variations in the thickness of the mantle transition zone. Using travel times of converted phases and SS precursors, the results of Lawrence and Shearer (2006) (**Figure 6(b)**) show systematic westward thickening of the transition zone in the Pacific, correlating with increasing plate age. This could imply temperature variations associated with convective instabilities beneath cooling plates may extend to depths of at least the top of the transition zone, ~440 km depth.

The G discontinuity is an important feature of the oceanic upper mantle seismic velocity structure that has been detected using reflected and converted body waves. A recent review is given by Rychert et al. (2012). Early work of Gaherty et al. (1996, 1999) and Tan and Helmberger (2007) examined propagation paths in the Pacific shown in **Figure 4(b)**. **Figure 4(b)** also shows shear wave velocity profiles inferred from the analysis of waveforms for propagation along these paths. The G discontinuity at a depth of about 60 km is a prominent feature of the modeled variation of shear wave velocity with depth, defining the top of the low-velocity asthenosphere. This feature has thus often been thought to coincide with the lithosphere–asthenosphere boundary. Using a combination of ScS, multiple S bounces, and surface waves (Gaherty et al., 1999; Tan and Helmberger, 2007), this G discontinuity appears to be due to a sharp (<30 km thick) 6% velocity decrease at relatively constant depth (60 ± 20 km) across a large transect of the central Pacific. More recently, a number of seismic tools including receiver functions, SS precursors, and velocity inversions using waveform modeling of multiple S reflections have also detected a shallow upper mantle seismic discontinuity in the Pacific Ocean. However, these methods give different results in both magnitude and thickness of the 'discontinuity' and where it is detected. High-frequency SS precursors (Schmerr, 2012) detect a sharp (<20 km thick) velocity decrease (≥5%) showing a weak age dependence (~55–75 km) primarily beneath hot spot regions but not elsewhere. ScS reverberations detect a sharp (<30 km thick) velocity decrease (5–14%) at 72–112 km depth beneath a large swaths of the western Pacific but not in the eastern Pacific (Bagley and Revenaugh, 2008). Receiver function imaging of subducting oceanic lithosphere reveals a sharp (<15 km thick) discontinuity (7–8%) (Kawakatsu et al., 2009) in the 44–85 km depth range (Kawakatsu et al., 2009; Kumar and Kawakatsu, 2011), which is imaged on the old Pacific and younger Philippine Sea Plate. A discontinuity at 25–130 km depth is imaged beneath large portions of the Pacific, increasing in depth with crustal age (Rychert and Shearer, 2011). A sharp discontinuity is detected beneath young seafloor, but not necessarily everywhere. One possible explanation for these variable results may be the presence of anisotropic seismic velocity (Rychert et al., 2012). Previous methods applied considering waves propagating at different azimuths show propagation direction variation in the inferred velocity structure. Anisotropy may thus be an important factor in imaging and constraining discontinuity structure in the oceanic upper mantle. It will be important to consult recent publications in the rapidly developing area.

Seismic anisotropy (Mainprice, Vol. 2; Park Vol. 1) in the upper mantle also provides a possible indication of mantle flow and could have important implications for understanding convective instability. Azimuthal anisotropy has been long recognized (cf. Montagner and Tanimoto, 1991; Nishimura and Forsyth, 1989), but its depth variation and the relative contributions from the lithosphere and asthenosphere are not yet resolved. In a simple unidirectional parallel flow, the seismic fast direction is usually assumed to lie close to the shear plane and in the flow direction. In more complex flows, the seismically fast direction has been assumed to coincide with the local direction of maximum accumulated elongation. However, the strength and local direction of anisotropy will be determined by the rates at which preferred orientation of mineral grains is created and destroyed by shear and dynamic recrystallization, respectively (Chastel et al., 1993; Kaminski and Ribe, 2001, 2002; Wenk and Tomé, 1999). Several recent global tomography studies have also reported radial anisotropy that is more pronounced beneath the Pacific Plate than elsewhere in the oceanic upper mantle (e.g., Ekstrom and Dziewonski, 1998; Gaboret et al., 2003; Nettles and Dziewonski, 2008). Could this radial anisotropy be a consequence of seismically fast directions vertically aligned in the upwellings and downwellings of convective motion? Hopefully, questions of this type can be resolved by continuing study.

The origin of the seismically defined low-velocity, high-attenuation asthenosphere is not fully resolved (Stixrude, Vol. 2). The possible effects of small amounts of melt (Boehler, Vol. 2) have been frequently discussed, but recent studies indicate that the presence of melt may not be required (Priestly and McKenzie, 2006; Stixrude and Lithgow-Bertelloni, 2006a,b) based on the new understanding of factors controlling shear wave velocities at seismic frequencies now emerging. Stress relaxation at grain boundaries is thought to be an important anharmonic effect that introduces a frequency–grain size variation and a temperature dependence to the elastic moduli in addition to that of high-frequency (harmonic) variations with temperature and pressure (Cooper, 2002; Faul and Jackson, 2005; Gribb and Cooper, 1998; Jackson et al., 2002). Variations in grain size and water content could thus contribute to the velocity variation with depth like those shown in **Figure 4**.

Explaining the origin of the G discontinuity has been a recent focus of interest. The presence of this seismic

discontinuity could have important implications for the origin of the asthenosphere. While seismic velocity decreases with increasing temperature, temperature gradients at the top of the asthenosphere are generally expected to be too small to explain the small width of the G discontinuity. Three different mechanisms have been discussed for the origin of the G discontinuity and perhaps the asthenosphere beneath it: (a) variations of seismic velocity with grain size and water content, (b) the development or changing directions of seismic anisotropy with depth, and (c) the presence of small amounts of melt.

Increased seismic attenuation in the asthenosphere may account for the reduced seismic velocity there, as discussed earlier. But whether attenuation can explain the rapid variation of velocity with depth required to create the G discontinuity is less clear. Karato (2012) provided a recent review of possible mineral physics mechanisms that may be responsible for seismic velocity variations. Seismic velocity is controlled by anharmonic (elastic) and anelastic mechanisms. The dependence on temperature and pressure for the anharmonic component is well known. Anelastic mechanisms are due to frequency-dependent attenuation that lowers seismic velocity. At high frequency, anelastic relaxation by elastically accommodated grain boundary sliding is characterized by a sharp peak at a particular frequency. At lower frequency, a diffuse absorption band is caused by diffusional accommodation of elastic stresses by grain boundary sliding. The frequency of the absorption peak is expected to increase with water content and temperature, although this has not yet been fully verified by experiments. The hypothesis proposed by Karato (2012) for the origin of the G discontinuity is then: in the cool and dry lithosphere, the absorption peak occurs at a frequency exceeding that of seismic body waves so that the shear modulus is unrelaxed (corresponding to high velocity), whereas in the asthenosphere, the absorption peak occurs at a frequency below that of seismic shear waves. The absorption band behavior has been documented in laboratory studies (Jackson and Faul, 2010; Sundberg and Cooper, 2010). Further study will be needed to confirm the suggested behavior of the absorption peak.

As described earlier, radial and azimuthal seismic anisotropies of the uppermost mantle are well documented. Azimuthal anisotropy may change direction with depth: fast direction in the lithosphere and asthenosphere in the direction of plate spreading and the direction of plate motion, respectively. It remains to be understood whether changes in the strength or direction of anisotropy with depth can be sufficiently rapid to explain the G discontinuity (e.g., Fischer et al., 2010).

7.08.2.5 Upper Mantle Electrical Conductivity: Water Content and Temperature

Long-period magnetotelluric studies of mantle electrical structure beneath the eastern North Pacific Ocean can detect electrical conductivity structure between 150 and 1000 km (Lizarralde et al., 1995). Interpretation of these data reveals a conductive zone between 150 and 400 km in depth with continuously decreasing conductivity at greater depth. Mantle conductivity in this region is comparable to that in the Basin and Range Province and much higher than that in the Canadian Shield. High conductivities could be explained by the presence of gravitationally stable partial melt. Alternatively, conductivity estimates on measurements of hydrogen solubility and diffusivity in olivine can explain the high conductivities observed. This reinforces the possible role of water in controlling the physical properties, and particularly the rheology, of the upper mantle (Hirth and Kohlstedt, 1996; Hirth et al., 2000). Several recent studies measuring the electrical conductivity of wet olivine (Wang et al., 2006; Yoshino et al., 2006) reach opposing conclusions on whether intragranular water (H defects) alone can explain observed conductivities or whether partial melt is required.

7.08.2.6 The Age of Thermal Convective Instability Beneath Oceanic Lithosphere

Global gravity anomaly maps (Jekeli, Vol. 3) derived from Seasat altimetry data display gravity lineations in the Pacific with 150–200 km wavelength aligned in the direction of plate motion (Haxby and Weissel, 1986) as shown in **Figure 5**. Haxby and Weissel (1986) suggested that these gravity lineations were a consequence of mantle convection currents organized by plate motions. In a sheared fluid layer with an initial linear temperature gradient, corresponding to heating from below and cooling from above, convective instability takes the form of convective rolls aligned with plate motion (Richter, 1973; Richter and Parsons, 1975). The presence of gravity lineations due to convective instability beneath lithosphere only a few million years old contrasted with the view that convective instability at ages ~70 My explained the flattening of old seafloor.

Motivated by the observed gravity anomalies, numerical studies of steady-state finite amplitude thermal convection showed that convective instability at young ages could be consistent with mantle thermally activated creep rheology (Buck, 1985) and estimated the convective heat fluxes required to explain the observed gravity anomalies (Lin and Parmentier, 1985). Numerical solutions for the development of thermal convection in a fluid layer cooled from above, with a plausible range of rheological parameters, predicted the effect of convective instability on geophysical observables (Buck and Parmentier, 1986). This study assumed that stresses generated by cool mantle sinking from the bottom of the unstable thermal boundary layer did not contribute to seafloor topography and resulting geoid anomalies, implying that this negatively buoyant mantle was supported by higher-viscosity mantle at depth. Robinson and Parsons (1988) showed that this is a reasonable approximation if mantle viscosity increases sufficiently with depth. If this were not so, convective instability, which increases the rate of cooling of mantle columns, would cause more rapid seafloor subsidence rather than reduced subsidence as previously assumed (cf. O'Connell and Hager, 1980). The calculated geoid anomaly showed a rapid decline in the geoid–age slope as convective instability developed and compared favorably to observed variations in geoid slope with age as shown in **Figure 3**. Other more recent studies argue that convective motions that develop at young ages may explain depth and geoid–age data better than plate model advocates have assumed. Doin and Fleitout (1996) showed that a uniform heat flux supplied to the bottom of the thermal boundary layer, presumably by convective motions, explains depth–age

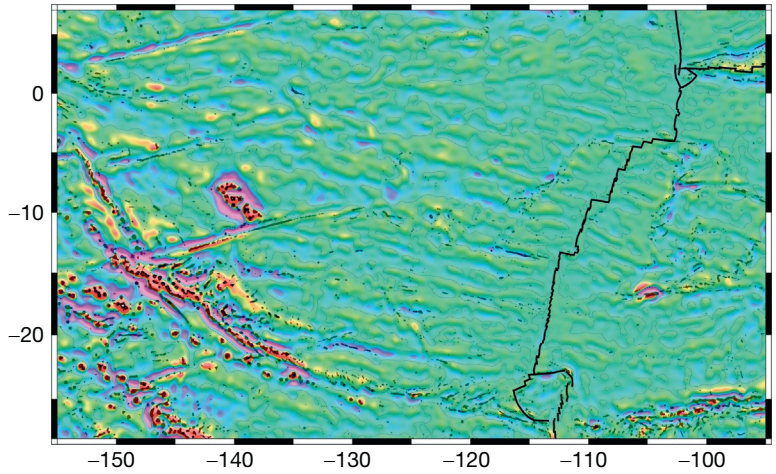

Figure 5 Haxby gravity lineations depicted in this satellite gravity image by Sandwell and Fialko (2004). Band-pass filtered gravity anomaly ($80 < \lambda < 600$ km) derived from retracked satellite altimeter data. Color scale saturates at ± 15 mGal. Gravity lineations with 140 km wavelength develop between the ridge axis and 6 Ma and are oriented in the direction of absolute plate motion. Lineations on older seafloor have somewhat longer wavelength (~180 km) and cross the grain of the seafloor spreading fabric. Gravity lineations also occur on the Nazca Plate to the east of the East Pacific Rise.

and plate model and also the rapid decline in the geoid–age slope at young ages.

Haxby and Weissel (1986) suggested the presence of longer wavelengths of small-scale convection beneath older regions of the Pacific. Wessel et al. (1996) identified gravity undulations with wavelengths of ~280 and 1000 km that form small circles about the current pole of Pacific Plate motion. The shorter wavelengths would correspond to the Haxby gravity lineations. The longer wavelengths could reflect the spacing of hot spot tracks or a larger scale of thermal boundary convective instability corresponding to that usually invoked to explain the plate model. The earlier study of Cazenave et al. (1995) had also indicated a wavelength of about 1000 km. Mantle seismic tomography using ray paths along a profile connecting Tonga and Hawaii identified seismic velocity anomalies with a spacing of about 1500 km that correlated with variations in gravity and bathymetry (Katzman et al., 1998). As the depth of a convectively cooled mantle layer increases with time, simple dimensional and scaling arguments suggest that the wavelength of convective motions should increase, a behavior seen in early studies of convective instability (Buck and Parmentier, 1986), but more recent studies, summarized in the succeeding text, further address this.

The Haxby gravity lineations are subtle features of the gravity field, generally much smaller than gravity anomalies due to fracture zones, for example. The current Pacific and Nazca Plate motion is oblique to fracture zones so that lineations aligned with plate motion cut obliquely across them. For other plates that move nearly parallel to fracture zones within them, gravity lineations of comparable amplitude to those in the Pacific would be difficult to detect, so that to identify convective instability at young ages requires other evidence. If convective instability occurs beneath the fast moving Nazca and Pacific Plates, does it also occur beneath more slowly moving plates created by slower spreading? As discussed earlier, Sandwell and Schubert (1980) found that geoid height for the Atlantic and southeast Indian spreading centers decreases approximately linearly with age with a geoid–age slope comparable to that expected for purely conductive cooling. This suggests that small-scale convective instability at young ages does not occur beneath these more slowly spreading plates.

Previous studies have often treated either hot spots or small-scale convective instability as the mechanism of lithospheric heating in all ocean basins. However, one mechanism of heat transfer need not be responsible for heating the lithosphere everywhere. With due caution concerning the nonlinearity of thermal convection (meaning that simply adding heat fluxes due to hot spots and small-scale convection may not be valid), it may even be reasonable to think that both mechanisms operate simultaneously but to different degrees beneath different ocean basins. Gravity lineations at young ages are visible only on the Pacific and Nazca Plates, suggesting that convective instability at young ages may develop under these fast moving plates. In the South Atlantic, where hot spot tracks are sparse and gravity lineations are not detectable, square root of age subsidence to ages exceeding 100 My would be consistent with purely conductive mantle cooling beneath this slower moving plate.

7.08.2.7 Implications from Recent Theoretical and Experimental Studies of Convective Instability

Convective instability of a thermal boundary layer has been examined in numerous studies using a range of analytic methods (see, e.g., Yuen and Fleitout, 1984; Marquart et al., 1999) and both laboratory (00003, this volume) and numerical experiments (00003 and 00005, this volume; Zaranek and Parmentier, 2004), the latter taking advantage of advances in computer speed and memory, to better understand the development of convective instability in a time-dependent basic state (conductive cooling) and temperature-dependent viscosity. The strong temperature dependence of mantle viscosity presents a significant challenge for numerical experiments and emphasizes the important continuing role of laboratory experiments.

Davaille and Jaupart (1994) derived scaling laws for convective onset time (age) and heat flow in a viscous fluid with strongly temperature-dependent viscosity cooled from above.

A convective heat flux f independent of the depth of the convecting fluid, implying that the boundary thickness is small compared to the fluid depth, is given by

$$f = Ck\left(\frac{\rho\alpha g}{\mu\kappa}\right)^{1/3}\Delta T_c^{4/3}$$

where k, κ, α, and ρ are the thermal conductivity, thermal diffusivity, thermal expansion coefficient, and density, respectively, and $C = 0.16$ is a dimensionless constant determined from laboratory or numerical experiments. This expression for the heat flux follows directly from dimensional analysis. Davaille and Jaupart (1994) showed that the convecting thermal boundary layer coincided with a tenfold increase in viscosity, corresponding to temperature decrease ΔT_c. For thermally activated creep,

$$\mu = \mu_m \exp\left[\frac{Q}{R}\left(\frac{1}{T} - \frac{1}{T_m}\right)\right]$$

where μ_m and T_m correspond to the temperature and viscosity beneath the thermal boundary layer. Then,

$$\Delta T_c = 2.24\frac{RT_m^2}{Q}$$

This heat flux scaling and the values of C are also confirmed by numerical experiments (Grasset and Parmentier, 1998). Heat flux as a function of μ_m and Q is shown in Figure 6. In the mantle, a heat flux due to small-scale convection comparable to that which would be required by the plate model ($\sim$40 mW m^{-2}) and creep activation energies from $Q = 250$ to 600 kJ mol^{-1} would require asthenosphere viscosities between 3×10^{18} and 4×10^{17} Pa s.

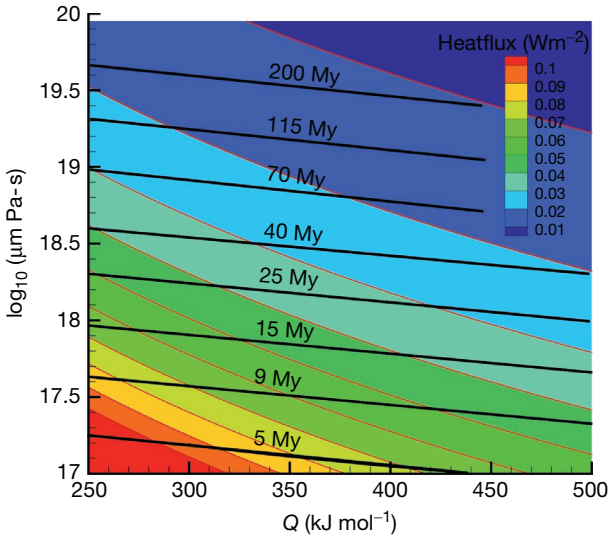

Figure 6 Contours of mantle heat flux beneath old oceanic lithosphere (based on heat flux scaling of Davaille and Jaupart (1994)) and onset time (age) of convective instability (reproduced from Zaranek SE and Parmentier EM (2004) Convective instability of a fluid with temperature-dependent viscosity cooled from above. *Earth and Planetary Science Letters* 224: 371–386) as a function of mantle viscosity and activation energy for thermally activated creep. For mantle heat flow below old oceanic crust of $\sim$50 mW m^{-2} (see Figure 2), onset of convection at young ages should occur if the creep activation energy is sufficiently high and mantle viscosity sufficiently low.

The small scale of thermal structures and convective motions in the mantle predicted by laboratory and numerical experiments is important to appreciate. For a convective heat flux beneath old lithosphere of $\sim$40 mW m^{-2} and $\Delta T_c \sim 100\,^{\circ}$C, the convecting thermal boundary layer thickness $\delta_c \sim k\Delta T_c/f$ is < 10 km, and convective instability of the boundary layer is expected to generate cold downwellings of comparable width.

The onset time of convective instability can also be determined from both laboratory and numerical experiments. For $Q = 250$ kJ mol^{-1} and a mantle temperature of 1300 °C, Davaille and Jaupart predicted the onset time from their laboratory-derived scaling to be in the range 52–65 My. High-resolution numerical experiments examining the onset of convection in a fluid with strongly temperature-dependent viscosity have been reported in several recent studies (Huang et al., 2003; Korenaga and Jordan, 2003a; Zaranek and Parmentier, 2004). These studies predict shorter onset times than earlier studies. Since convective motions, even those restricted to the upper mantle, must allow for scales as large as 1000 km, the small scales of convective instability indicated earlier would be difficult to resolve numerically. An understanding of the scaling of onset time with temperature dependence is needed to extrapolate well-resolved numerical experiments to the very stronger temperature dependence of viscosity expected in the mantle. Recent numerical experiments, which are all in good agreement with each other, indicate a scaling for onset time that differed from that proposed by Davaille and Jaupart (2004). The onset time scaling of Zaranek and Parmentier (2004), for example, leads to the predictions shown in Figure 6.

In Figure 6, contours of heat flux provided to the base of the conductive lithosphere by small-scale convection in color shading and onset time in solid contours are plotted as a function of the creep activation energy Q and mantle viscosity μ_m beneath the thermal boundary layer. The upper mantle viscosity beneath spreading centers and areas of active plate extension such as the North American Basin and Range Province is not expected to exceed about 10^{19} Pa s (Bills, 1994; Passey, 1981; Sigmundsson, 1991). Estimates based on laboratory rheological measurements suggest an even lower viscosity of 10^{18} Pa s (Hirth and Kohlstedt, 1996). If small-scale convection provides all the heat flux to old seafloor ($\sim$45–50 mW m^{-2}; see Figure 2) and if an upper mantle viscosity of 10^{18} Pa s is assumed, convective instability would occur at ages of $\sim$15 My for $Q = 350$–400 kJ mol^{-1}, values intermediate between diffusion ($\sim$300 kJ mol^{-1}) and dislocation creep ($\sim$500 kJ mol^{-1}) in olivine.

The onset of convection at ages $\leq$10 My would require μ_m below 10^{18} Pa s and Q near the value for dislocation creep in olivine. For convective instability at 70 My with a convective heat flux of 40 mW m^{-2}, a value of μ_m higher than those cited earlier would be required with a creep activation energy lower than 300 kJ mol^{-1}. For Q within the 300–500 kJ mol^{-1} range, onset of convection in the 50–70 My age range would be

possible only with an upper mantle viscosity of 10^{19} Pa s and then only if the convective heat flux due to small-scale convection beneath old seafloor were $\leq$30 mW m^{-2}. This may be possible if small-scale convection transports only a fraction of the heat needed to explain the surface heat flow and bathymetry of old seafloor, the remainder being due to heating of the lithosphere at hot spots, as discussed earlier.

Mantle viscosity μ_m may differ near a spreading center and beneath older seafloor. Near spreading centers, the presence of melt may reduce viscosity. Conversely, since the presence of intragranular water in nominally anhydrous minerals reduces creep viscosity and water is a relatively incompatible element, the extraction of melt may dehydrate the mantle, thus increasing viscosity (Hirth and Kohlstedt, 1996; Karato, 1986). As discussed in the succeeding text, the latter effect may be the more dominant one, depending on the sensitivity of creep rates to water content and the water content of the mantle prior to melting.

As indicated earlier, convective instability at young ages may be present only beneath the Nazca and Pacific Plates, which are both fast moving and formed at a high spreading rate. Why might convective instability at young ages be restricted to fast spreading or fast moving plates? Is spreading rate or plate velocity the determining factor? Slower spreading rates should lead to a thicker thermal boundary layer beneath the spreading axis, thus promoting convective instability at younger ages (Sparks and Parmentier, 1993). Other possible effects of spreading rate are discussed later. The linear stability analysis of Korenaga and Jordan (2003b) indicates that convective rolls aligned with plate motion may be stable only in the presence of strong shearing beneath fast moving plates. However, rheological effects may also be important. Beneath fast moving plates, higher strain rates could create smaller grain size resulting in more rapid diffusion creep with lower μ_m or higher stresses resulting in deformation dominated by dislocation creep with higher Q. As shown in **Figure 6**, both lower μ_m and higher Q would favor convective instability at younger ages. Rising mantle that is enriched in water relative to that in other regions might also explain a lower mantle viscosity beneath the EPR, thus promoting early onset times.

The scale or wavelength of small-scale convection appears to increase to $\geq$1000 km beneath the old Pacific seafloor. Korenaga and Jordan (2004) recently examined how the horizontal scale of convective motions in a fluid with temperature- and depth-dependent viscosity would increase with age, including in particular the effect of an endothermic phase transition at the base of the upper mantle. They suggested that convection initiated at small scales beneath moving plates could eventually penetrate the stable phase transition and evolve into whole mantle convection.

All of the studies discussed earlier treat the development and evolution of convective motions as two-dimensional (2D) and time-dependent, most closely approximating convective motions in a vertical plane orthogonal to plate motion as a function of plate age. Despite significant advances in both computer speed and numerical methodologies, fully three-dimensional treatments of thermal convection with the very strongly temperature-dependent viscosities believed to characterize mantle flow remain challenging (see 00005, this volume). Numerical solutions must simultaneously resolve 10 km thick thermal boundary layer layers and cold plumes embedded in several thousand kilometer-scale flow.

van Hunen et al. (2003) studied 3D convective instability beneath a moving plate. In agreement with earlier analysis, plate motion enhanced the development of longitudinal convective rolls relative to motion-perpendicular transverse rolls. They found that the onset age of fully 3D convective motions was similar to that in earlier 2D studies. It would be interesting to more closely examine the evolution of convective motions with age, in particular how the scale or wavelength of convective motions increases as cooling proceeds. A first impression based on van Hunen et al. (2003) (**Figure 1**) suggests that the scale of convective motions does not increase as rapidly as suggested by earlier 2D studies.

7.08.3 Convective Instability and Melting in the Upper Mantle

7.08.3.1 Intraplate Volcanism as an Indicator of Upper Mantle Convective Activity

Volcanism away from plate boundaries (00009, this volume; McNutt, Vol. 1) is generally thought to be a consequence of decompression melting due to convective motions that arise from deeper in the mantle or from instability generated in the upper mantle. Linear, long-lived, and age-progressive volcanic chains have been explained as the manifestation of fixed hot spots, possibly generated by buoyant plumes of rising material (00009, this volume) originating deep in the mantle (Morgan, 1971). While the Wilson–Morgan fixed hot spot model has been successfully applied to volcanic chains in all ocean basins, important disagreements have been recognized between geochronological observations and the simplest predictions of the model. For example, Okal and Batiza (1987) and McNutt (1998) outlined numerous examples where the fixed hot spot model fails to explain (a) observed departures from linearity of individual volcanic chains and inconsistent orientations among multiple chains that lie on the same plate, (b) short-lived chains and ones that fluctuate in size, and (c) violations of predicted age-progressive behavior. For example, the Cook–Austral Chain (Turner and Jarrard, 1982) and the Line Islands (Schlanger et al., 1984) exhibit complex age progressions with volcanic activity occurring along multiple lineaments and with volcanoes of distinctly different ages in close proximity to one another. Furthermore, some linear volcanic ridges in the Pacific form much more rapidly than would be predicted by fixed hot spot model (Bonatti et al., 1977; Sandwell et al., 1995).

The creation of large igneous provinces (00010, this volume) or oceanic plateaux by partial melting of the starting plume head is a corollary of the mantle plume hypothesis for the origin of hot spots (Richards et al., 1989). Of the 14 possible Pacific hot spot tracks studied by Clouard and Bonneville (2001), only 3 (Louisville, Easter, and Marquesas) can be traced to an oceanic plateau. Seven hot spots have short tracks $<$35 My and clearly cannot be traced to an oceanic plateau. Koppers et al. (2003) found that linear volcanic chains in the western Pacific and South Pacific Superswell region typically display intermittent volcanic activity with longevities shorter than 40 My, superposed volcanism, and motion

relative to other longer-lived hot spots. Finally, study of marine satellite gravity data in the Pacific (Wessel and Lyons, 1997) shows the presence of many volcanoes with a range of sizes in a variety of geologic settings. Most of these volcanoes do not clearly align in chains or ridges, and most seem too small to be explained by deep mantle plumes. While the long-lived age-progressive volcanic chains that fit the fixed hot spot model are remarkable features, other mechanisms of intraplate volcanism must also be active (see also 00010, this volume).

7.08.3.2 Other Possible Mechanisms for Intraplate Volcanism

Diffuse plate extension (Sandwell et al., 1995) has been frequently cited as a possible mechanism of intraplate volcanism. Proposed partly on morphological grounds, this mechanism was thought to explain rapid propagation of volcanic ridges and the formation of volcanic ridges in troughs of topography associated with the Haxby gravity lineations. Volcanism was thought to be attributable either to allowing melt already present in the upper mantle access to the surface or to decompression melting in upwellings associated with lithospheric boudinage. Dunbar and Sandwell (1988) calculated that 10% extension would be required for this mechanism. However, the amount of extension that can be allowed in the Pacific is $<1\%$ (Gans et al., 2003; Goodwillie and Parsons, 1992), seemingly much too small for significant boudinage. Thus, agreement seems to be emerging that the boudinage hypothesis does not satisfy available observations. An interesting alternative is cracking of the lithosphere under the action of thermal contraction bending moments (Gans et al., 2003; Sandwell and Fialko, 2004). In this hypothesis, cracking of the plate allows lithosphere between cracks to bend, thus relieving thermal bending moments. Cracks form topographic troughs, and magma already existing beneath the lithosphere exploits these regions to reach the seafloor. Mantle seismic velocities beneath volcanic ridges formed in this way should be higher than in adjacent mantle, which does not seem to be the case, at least beneath the volcanic ridges where regional seismic data are available. Weeraratne et al. (2007) found lower seismic velocities, implying higher temperatures and/or more melt beneath these volcanic ridges. However, the ridges examined in this study are all near the East Pacific Rise spreading center on seafloor younger than 3 Ma. Seismic velocities beneath recently active volcanic ridges further from the spreading axis have not yet been studied in comparable ways.

7.08.3.2.1 Melting in convectively driven upwellings

Volcanism due to decompression melting in small-scale convective upwellings is perhaps the favored popular hypothesis for the origin of volcanic ridges aligned with plate motion (see also 00010, this volume). Melting in convective upwellings would be consistent with lower seismic velocities in the mantle beneath ridges. Buoyant convective upwellings should elevate the seafloor so that the resulting volcanism should occur on topographic highs. However, volcanic ridges were observed to lie in lows of the gravity lineations. If gravity lows correspond to topographic troughs, this would be inconsistent with a convective origin (Sandwell et al., 1995). However, seafloor topography with 100 m amplitudes over horizontal scales of several hundred kilometers is a subtle feature compared with the topography of volcanic constructs and the flexure caused by this loading. After removing lithospheric flexure due to the topographic loading, Harmon et al. (2006) found that volcanic ridges near the EPR actually lie on topographic highs. Topographic highs correspond to negative residual mantle Bouguer gravity anomalies that were obtained from the observed free-air anomaly by subtracting the effect of crustal thickness variations and the attraction of topography. If this relationship holds for other volcanic ridges, particularly those further from the EPR axis, then a convective origin for volcanic ridges and gravity lineations would be indicated. Harmon et al. (2011) argued for a convective origin based on the combined analysis of seismic velocity and density variations in the mantle.

7.08.3.2.2 Melting due to shear-driven upwelling

Decompression melting has frequently been associated with convectively driven mantle upwelling as discussed earlier. However, mantle upwelling due to plate motions and asthenospheric shear may also be driven by variation in plate thickness or by viscosity variations in a sheared asthenosphere. The fracture zones, across which seafloor age and thermal boundary layer thickness change abruptly, often move obliquely over the underlying mantle, providing one example of a setting in which upwelling can result from changes in plate thickness. Till et al. (2010) explored a recent model of this process in the context of a continental margin. Conrad et al. (2010) also presented models of mantle upwelling that results from lithosphere thickness variations.

Conrad et al (2010) also suggested that mantle upwelling may also result from viscosity variations in a sheared asthenosphere. Viscosity variations in the asthenosphere may be a consequence of preexisting variations in mantle composition, for example, water content, or the presence of melt. Conrad et al. (2011) presented evidence for a correlation between intraplate volcanic activity and rapid shearing of the asthenosphere. It is interesting to wonder how such viscosity variations in the asthenosphere might arise and the timescale on which they can be preserved. Volcanic chains near the East Pacific Rise spreading center, often attributed to upwelling in convective instability, provide an interesting example in which the space–time variation of volcanism may be due to the presence of fingers of low-viscosity mantle (Weeraratne et al., 2007) and upwelling due to asthenospheric shear in the presence of these viscosity variations (Ballmer et al., 2013). It is interesting to wonder if viscosity variations might arise spontaneously due to feedback between viscosity and melting.

7.08.3.3 Buoyant Decompression Melting

In addition to decompression melting in thermally driven convection, intraplate volcanism may be a product of decompression melting in convective upwellings that result from the buoyancy associated with melting itself (Hernlund and Tackley, 2003; Raddick et al., 2002; Tackley and Stevenson, 1993). This 'buoyant decompression melting' in a layer that is initially at its melting temperature may self-organize from small, initially random perturbations and thus might be termed 'magmatic convective storms.' Melt extraction leaves

behind a buoyant and creep-resistant residual mantle. The accumulation of this relatively immobile and infertile mantle ultimately limits the amount of melt that can be produced by the decompression melting mechanism (Raddick et al., 2002). This results in an inverse correlation between the rate of melt production and the duration of melting, which may be diagnostic of the buoyant decompression melting process.

Buoyant decompression melting could occur in a number of geologic settings; however, if the oceanic upper mantle has previously melted beneath a spreading center and subsequently cooled, spontaneous buoyant decompression melting may be possible only in regions where a large-scale mantle upwelling can counteract conductive cooling, keeping the mantle at its solidus temperature over some depth range. The South Pacific Superswell has been interpreted as a region of large-scale mantle upwelling (Gaboret et al., 2003; McNutt, 1998), and buoyant decompression melting may explain the abundance of volcanism associated with it. Alternatively, to balance the downward flux associated with sinking lithosphere, a small upward velocity should be present in large areas of the upper mantle away from convergent plate boundaries. Since transition zone mineral phases like the β- and γ-olivine have a larger water storage capacity than their lower pressure isomorph, upwelling mantle may dehydrate forming a water-rich melt above the transition zone (e.g., Bercovici and Karato, 2003). During the upward percolation of buoyant melt, as envisioned in an early study by Frank (1968), buoyant instabilities may lead to localization of melting, upwelling, and surface volcanism.

In the absence of a large-scale upwelling, where mantle is slightly cooler than its melting temperature, buoyant melting may not occur spontaneously but may be triggered by some initial upwelling due to relief on the bottom of the lithosphere, for example, across oceanic fracture zones that move obliquely across the mantle (e.g., Raddick et al, 2002). This may provide a physical explanation for intraplate volcanism that is controlled by lithosphere structure.

7.08.4 Upwelling and Melting Beneath Oceanic Spreading Centers

7.08.4.1 Melting, Melt Extraction, and the Chemical Lithosphere

Mantle upwelling and decompression melting beneath spreading centers (Jian Lin, Vol. 6) are expected to have important consequences for the development of convective motions as the lithosphere ages. Two effects may be particularly important: (a) melting and melt extraction are expected to affect both rheology and density and (b) convective instability beneath the spreading axis due to density variations associated with the presence of melt and its extraction from residual mantle may influence the scale and evolution of off-axis convective instability. Forsyth (1992) provided a relatively recent review of mantle flow beneath spreading centers; and the MELT Experiment (Forsyth et al., 1998) provides the best geophysical evidence on the amount and distribution of melt in the mantle beneath a very fast spreading section of the EPR. Geochemistry, for example, Lu–Hf systematics and U–Th disequilibrium, provides evidence that garnet was present during melting, thus providing a minimum estimate of ~70 km for the beginning of melting in upwelling mantle.

Hirth and Kohlstedt (1996) and Phipps Morgan (1997) pointed out that melting beneath spreading centers should produce a compositional lithosphere that is both more viscous, as mentioned earlier, and compositionally buoyant. Intragranular water that enhances the creep rate of nominally anhydrous mantle minerals behaves as a highly incompatible element during melting. The extraction of melt during fractional melting would leave behind a dry residual mantle. Removing essentially all the water present at concentrations inferred for upper mantle that melts beneath spreading centers may increase its viscosity by more than a factor of 100 (Hirth and Kohlstedt, 1996) (Kohlstedt, Vol. 2). The thickness of the residual layer should be comparable to the maximum depth of melting beneath a spreading center. Evans et al. (2005), using electrical conductivity, inferred a 60 km dehydration depth beneath a fast spreading section of the EPR (the MELT area at 17° S). The dehydrated residual mantle layer generated at a spreading center might be thought to correspond to the plate in the plate model seafloor evolution. However, this depth of dehydration appears significantly thinner than estimates of plate thickness in the range of 95–125 km discussed earlier. One possibility is that small amounts of wet melt form at the even greater depths comparable to the plate thickness. Interpretations of seismic data from the MELT Experiment do suggest small amounts of melting at depths exceeding 100 km (Forsyth et al., 1998).

7.08.4.2 Influence of Melt Extraction Mechanism

The rheological consequences of melt extraction should depend on the mechanism of melt migration. Does melt percolating upward remain distributed along mineral grain edges maintaining equilibrium with solid mantle as it goes? Or does it localize into larger channels after only small amounts of melt form? Melt that rapidly localizes into larger channels approximates ideal fractional melting that removes incompatible elements more effectively than equilibrium transport.

A fundamental observation is that the chemical composition of basalt erupted at spreading centers is not in equilibrium with residual mantle at low pressure (e.g., Elthon and Scarfe, 1984; O'Hara, 1965; Stolper, 1980). Melts must rise from depths of at least 30 km to the surface without extensive re-equilibration with surrounding mantle at shallow depth in order to preserve this deep geochemical signature. Focused melt flow through high-permeability conduits or channels is one possible mechanism. Several lines of evidence suggest that the porosity structure in the melt generation and extraction region of the mantle is heterogeneous consisting of interconnected high-porosity dunite channels embedded in a low-porosity harzburgite or lherzolite matrix (Kelemen et al., 1997 and references therein). Remnant dunite channels have been observed as veins, tabular or sometimes irregular-shaped bodies in ophiolites. These dunite dikes or veins make up 5–15% of the mantle in the Oman ophiolite with widths ranging from tens of millimeters to ~200 m and length from tens of meters to at least 10 km (Kelemen et al., 1997). Although their spatial distribution in the mantle is still not well constrained, the presence of a high-porosity,

interconnected, coalescing network of dunite channels present above or within the melting region has been envisioned. Porous flow through dunite channels is capable of producing observed Uranium-series disequilibriums and significant trace element fractionations during mantle melting and melt extraction (e.g., Kelemen et al., 1997; Lundstrom, 2003; Spiegelman and Elliott, 1993; Spiegelman and Kelemen, 2003).

At fast spreading rates, mantle upwelling and melting appear to occur over a several hundred kilometer wide region (e.g., Forsyth et al., 1998), but the oceanic crust is emplaced within a few kilometers of the spreading axis. Thus, a second major constraint on the mechanism of melt migration is that it must be capable of focusing melt to the spreading axis. If the viscosity of upwelling mantle is sufficiently high ($\geq 10^{20}$ Pa s), pressure gradients in the mantle flow may be sufficient to drive melt to the spreading axis (Phipps Morgan, 1987; Spiegelman and McKenzie, 1987). Alternatively, melt may migrate vertically to collect in a decompaction boundary layer that develops as melt begins to freeze. This should create a high-porosity melt channel that slopes away from the spreading axis providing a conduit for melt flow toward the axis (Sparks and Parmentier, 1991; Spiegelman, 1993). The first full numerical simulation of mantle upwelling melting and melt migration beneath a spreading center showing this decompaction boundary layer is shown in **Figure 7(a)** from Katz (2010). Rabinowicz and Ceuleneer (2005) suggested, in fact, that dunites in the Oman ophiolite may be the preserved remnants of this decompaction boundary layer. If melt in the decompaction layer is isolated in dunite channels, then some signature of high pressures will be preserved in the melts that accumulate near the spreading axis. However, melting need not be perfectly fractional so that mantle need not be fully dehydrated.

No seismic or electromagnetic evidence on the distribution of melting and upwelling in the mantle comparable to that for southern EPR is available for slower spreading centers. If buoyancy related to melting is important, then 'active' upwelling could lead to more localized melting at slow spreading rates. Active upwelling would produce higher, more uniform degrees of melting creating more strongly and uniformly dehydrated residual mantle less prone to convective instability. This is illustrated in **Figure 7** from Braun et al. (2000).

7.08.4.3 2D Versus 3D Upwelling and the Spreading Rate Dependence of Seafloor Structure

At slow spreading rates, buoyancy related to melting may also result in localized columns of upwelling and melting beneath the spreading axis (Choblet and Parmentier, 2001; Parmentier and Phipps Morgan, 1990). At high spreading rates, upwelling remains sheetlike along the spreading axis. This is one possible explanation for the difference in seafloor morphology and structure between fast and slow spreading centers and may also explain the strongly lineated morphology of seafloor produced at slow spreading rates (Phipps Morgan and Parmentier, 1995). At high spreading rates, buoyant decompression melting may produce off-axis upwelling columns that may explain near-axis volcanic ridges (Jha et al., 1997), providing a possible alternative to melting in thermally driven upwellings as discussed earlier.

7.08.5 Summary

The deviation of the age dependence of seafloor depth from predictions of a simple conductive thermal boundary layer (half-space cooling model) need not be explained by only a single mechanism. Both heating by hot spots and convective instability due to cooling from above may affect thermal evolution but differ in importance in different settings, for example, the North Atlantic and Pacific, respectively. Discussion has sometimes focused on which mechanism is the correct one rather than on assessing which may be more important and why. The relative importance of convective instability should depend on spreading rate and mantle composition, perhaps particularly through the effect of water on rheology.

The seafloor age at which convective instability begins clearly depends strongly on spreading rate and particularly mantle rheology. Convective instability at young ages remains a preferred explanation for gravity lineations on the Pacific and Nazca Plates but is not required beneath other plates. Beneath thicker, colder lithosphere at slow spreading centers, small-scale convection may be present but less visible. If small-scale convection is present beneath the fast spreading EPR but not beneath slower spreading centers, a number of explanations for this possible difference in behavior can be envisioned. The higher shear rates beneath rapid moving plates may organize convection into a lineated structure that is more visible in gravity data than other less organized patterns. Higher shear rates may also result in lower effective viscosity of the upper mantle beneath faster moving plates, therefore yielding earlier onset times.

The reduced rate of old seafloor has frequently been attributed to convective instability of the thermal boundary layer beneath a thickening conductive lid. If so, then convective instability would occur at ages of $\geq$70 My, which maintains a nearly uniform mantle temperature beneath the conductive lid. If elastic wave speed is primarily a function of temperature, an upper mantle temperature that does not decrease with seafloor age does not explain an elastic shear wave velocity, which seismic tomography indicates continues to increase with age. If elastic shear wave speed is reduced by the presence of intracrystalline water in nominally anhydrous mantle minerals, then small degrees of partial melting could increase seismic velocity through the extraction of water, which behaves as a relatively incompatible trace element. The presence of melt has also been suggested to explain the G discontinuity, which some studies suggest to be widespread in the oceanic upper mantle. However, other mechanisms to create the G discontinuity are under active consideration. The continuing increase in seismic velocity beneath seafloor with an old age and the presence of the G discontinuity seem likely to have important rheological implications that could improve our understanding of oceanic upper mantle convective instability.

Intraplate volcanism not associated with hot spots on the Pacific and Nazca Plates is much more abundant than in other ocean basins. Does this reflect an influence of deeper mantle processes or convective instability that develops within the upper mantle? The latter possibility would be broadly consistent with a lower-viscosity (higher strain rate, smaller grain size, and/or wetter) mantle beneath the Pacific and Nazca Plates than elsewhere in the upper mantle.

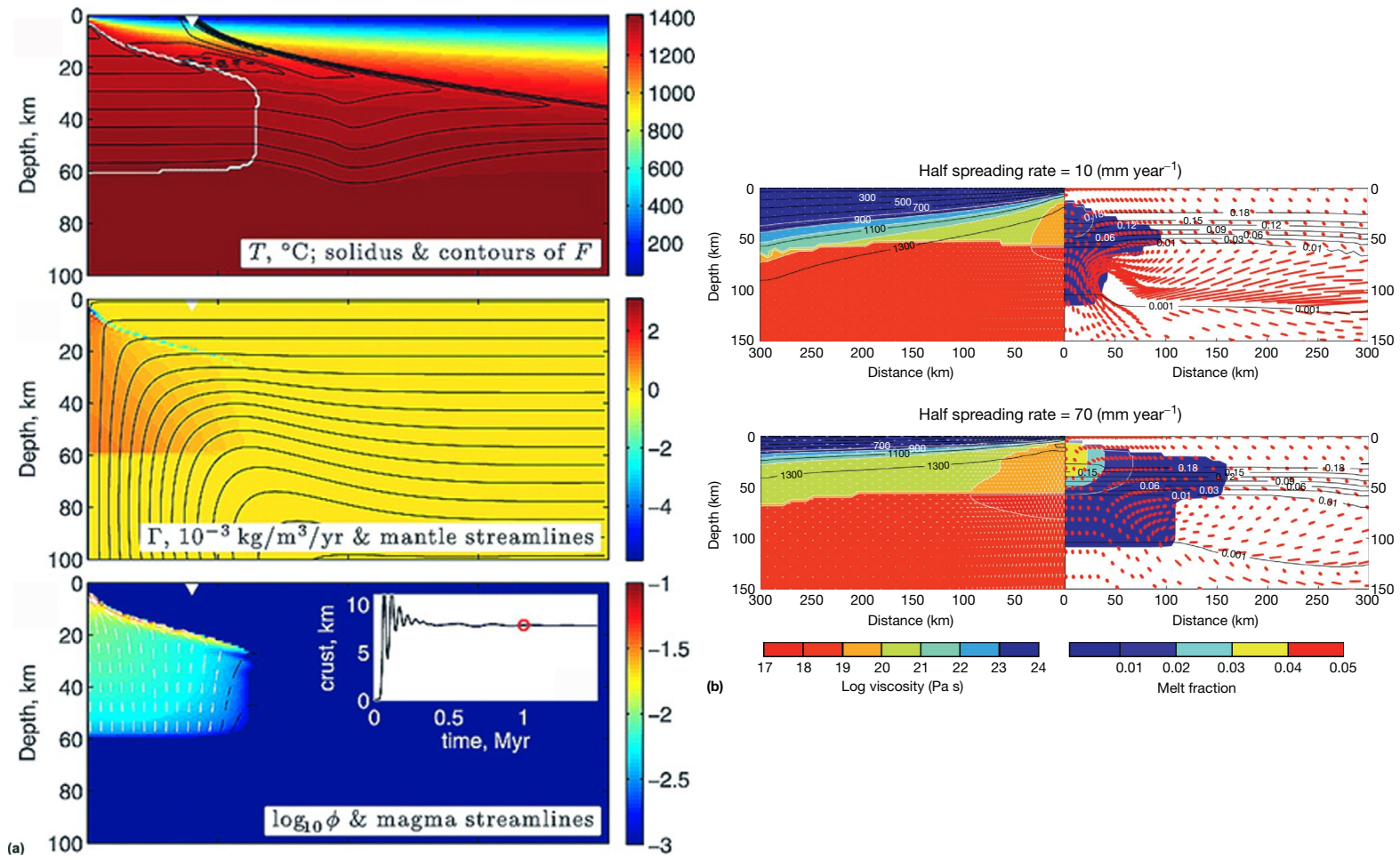

Figure 7 (a) Numerical simulation of mantle flow, melting, and melt migration beneath a spreading center with half spreading rate 4 cm year^{-1}, a mantle viscosity of 10^{18} Pa s, and potential temperature of 1375 °C from Katz (2010) illustrating the presence of a decompaction boundary layer. (top) Temperature, (middle) rate of melting, and (bottom) melt fraction present obtained from the simulation after 1 Ma of model time. White triangles show the distance of plate motion over this period. Black curves in top panel connect points of constant degree of melting, starting with 1% at the bottom of the melting region and increasing in steps of 2.5%; these lines cluster along the edge of the region that has experienced melting since spreading initiated. In this model, the maximum degree of melting is 20%. The inset in the bottom panel shows crustal thickness as a function of time. The red point marks the crustal thickness at 1 Ma. (b) Mantle upwelling and melting beneath fast and slow spreading centers from Braun et al. (2000). Solid contours in the left panel show the mantle viscosity, and black lines depict isotherms (at 200 °C intervals) for a potential temperature of 1350° and an adiabatic gradient of 0.3°C km^{-1}. Ellipses (red ovals) representing accumulated finite strain are plotted along solid flow streamlines corresponding to the velocity field shown by white vectors in the left panel. Solid contours on the right panel show the steady-state melt fraction (>0.1%) overlain by isodepletion contours (black lines). Rheology includes estimates of the effects of dehydration, melt, and grain boundary sliding with a reference viscosity of 5×10^{18} Pa s. Since the effects of dehydration dominate those of melt, the viscosity and velocity structures resemble more passive-like plate spreading flow above the dry solidus. Even with lower reference viscosities, buoyant flow is restricted to depths beneath the dry solidus. Buoyant localization of solid flow and melt generation at depth increases as the half spreading rate decreases. The magnitude and localization of strain also increase with decreasing spreading rate.

References

Ballmer MD, Conrad CP, Smith EI, and Harmon N (2013) Non-hotspot volcano chains produced by migration of shear-driven upwelling toward the East Pacific Rise. *Geology* 41: 479–482. http://dx.doi.org/10.1130/G33804.1.

Bercovici D and Karato S (2003) Whole-mantle convection and the transition-zone water filter. *Nature* 425: 39–44. http://dx.doi.org/10.1038/nature01918.

Bills BG (1994) Viscosity estimates for the crust and upper mantle from patterns of lacustrine shoreline deformation in the eastern Great Basin. *Journal of Geophysical Research* 99: 22059–22086.

Bonatti E, Harrison CGA, Fisher DE, et al. (1977) Easter volcanic chain (southeast Pacific): A mantle hotline. *Journal of Geophysical Research* 82: 2437–2478.

Braun M, Hirth G, and Parmentier EM (2000) Effects of deep damp melting on mantle flow and melt generation beneath mid-ocean ridges. *Earth and Planetary Science Letters* 176: 339–356.

Buck WR (1985) When does small scale convection begin beneath oceanic lithosphere? *Nature* 313: 775–777.

Buck WR (1987) Analysis of the cooling of a variable-viscosity fluid with applications to the Earth. *Geophysical Journal of the Royal Astronomical Society* 89: 549–577.

Buck WR and Parmentier EM (1986) Convection beneath young oceanic lithosphere: Implications for thermal structure and gravity. *Journal of Geophysical Research* 91: 1961–1974.

Carlson RL and Johnson HP (1994) On modeling the thermal evolution of the oceanic upper mantle: An assessment of the cooling plate model. *Journal of Geophysical Research* 99(B2): 3201–3214. http://dx.doi.org/10.1029/93JB02696.

Cazenave A (1984) Thermal cooling of the oceanic lithosphere: New constraints from geoid height data. *Earth and Planetary Science Letters* 70: 395–406.

Cazenave A, Lago B, and Dominh K (1982) Geoid anomalies over the north-east Pacific fracture zones from satellite altimeter data. *Geophysical Journal* 69: 15–31.

Cazenave A, Lago B, and Dominh K (1983) Thermal parameters of the oceanic lithosphere estimated from geoid height data. *Journal of Geophysical Research* 88: 1105–1118.

Cazenave A, Parsons B, and Calcagno P (1995) Geoid lineations of 1000-km wavelength over the central Pacific. *Geophysical Research Letters* 22: 97–100.

Chase CG (1985) The geological significance of the geoid. *Annual Review of Earth and Planetary Sciences* 13: 97–117.

Chastel YB, Dawson PR, Wenk H-R, and Bennett K (1993) Anisotropic convection with implications for the upper mantle. *Journal of Geophysical Research* 98: 17757–17772. http://dx.doi.org/10.1029/93JB01161.

Choblet G and Parmentier EM (2001) Mantle upwelling and melting beneath slow spreading centers: Effects of variable rheology and melt productivity. *Earth and Planetary Science Letters* 184: 589–604.

Clouard V and Bonneville A (2001) How many Pacific hotspots are fed by deep-mantle plumes? *Geology* 29: 695–698.

Colin P and Fleitout L (1990) Topography of the ocean floor: Thermal evolution of the lithosphere and interaction of the deep mantle heterogeneities with the lithosphere. *Geophysical Research Letters* 17: 1961–1964.

Conrad CP, Benjun W, Smith EI, Bianco TA, and Tibbetts A (2010) Shear-driven upwelling induced by lateral viscosity variations and asthenospheric shear: A mechanism for intraplate volcanism. *Physics of the Earth and Planetary Interiors* 178(3): 162–175.

Conrad CP, Bianco TA, Smith EI, and Wessel P (2011) Patterns of intraplate volcanism controlled by asthenospheric shear. *Nature Geoscience* 4: 317–321.

Cooper RF (2002) Seismic wave attenuation: Energy dissipation in viscoelastic crystalline solids. In: Karato S and Wenk H-R (eds.) *Plastic Deformation of Minerals and Rocks*. Washington, DC: Mineralogical Society of America.

Craig CH and McKenzie DP (1986) The existence of a thin low-viscosity layer beneath the lithosphere. *Earth and Planetary Science Letters* 78: 420–426.

Crosby AG and McKenzie D (2009) An analysis of young ocean depth, gravity and global residual topography. *Geophysical Journal International* 178: 1198–1219.

Crosby AG, McKenzie D, and Sclater JG (2006) The relationship between depth, age and gravity in the oceans. *Geophysical Journal International* 166: 553–573.

Crough ST (1975) Thermal model of oceanic lithosphere. *Nature* 256: 388–390.

Crough ST (1977) Approximate solutions for the formation of the lithosphere. *Earth and Planetary Science Letters* 14: 365–377.

Crough ST (1978) Thermal origin of mid-plate hot-spot swells. *Geophysical Journal of the Royal Astronomical Society* 55: 451–469.

Crough ST (1979a) Geoid anomalies across fracture zones and the thickness of the lithosphere. *Earth and Planetary Science Letters* 44: 224–230.

Crough ST (1979b) Hotspot epeirogeny. *Tectonophysics* 61: 321–333.

Davaille A and Jaupart C (1994) One onset of thermal convection in fluids with temperature-dependent viscosity: Application to the ocean mantle. *Journal of Geophysical Research* 99: 19853–19866.

Davis EE and Lister CRB (1974) Fundamentals of ridge crest topography. *Earth and Planetary Science Letters* 21: 405–413.

Detrick RS (1981) An analysis of geoid anomalies across the Mendocino fracture zone: Implications for thermal models of the lithosphere. *Journal of Geophysical Research* 86: 11751–11762.

Detrick RS and Crough ST (1978) Island subsidence, hot spots and lithosphere thinning. *Journal of Geophysical Research* 83: 1236–1244.

Doin MP and Fleitout L (1996) Thermal evolution of the oceanic lithosphere: An alternative view. *Earth and Planetary Science Letters* 142: 121–136.

Doin M-P, Fleitout L, and McKenzie D (1996) Geoid anomalies and the structure of continental and oceanic lithospheres. *Journal of Geophysical Research* 101: 16119–16136. http://dx.doi.org/10.1029/96JB00640.

Driscoll ML and Parsons B (1988) Cooling of the oceanic lithosphere – Evidence from geoid anomalies across the Udintsev and Eltanin fracture zones. *Earth and Planetary Science Letters* 88: 289–307.

Dunbar J and Sandwell D (1988) A boudinage model for cross-grain lineations (abs.). *EOS, Transactions, American Geophysical Union* 69: 1429.

Eberle MA and Forsyth DW (1995) Regional viscosity variations, small-scale convection and the slope of the depth-age ½ curve. *Geophysical Research Letters* 22: 473–476.

Ekstrom G and Dziewonski AM (1998) The unique anisotropy of the Pacific upper mantle. *Nature* 394: 168–172.

Elthon D and Scarfe CM (1984) High-pressure phase equilibria of a high-magnesia basalt and the genesis of primary oceanic basalts. *American Mineralogist* 69: 1–15.

Evans RL, Hirth G, Baba K, Forsyth D, Chave A, and Mackie R (2005) Geophysical evidence from the MELT area for compositional controls on oceanic plates. *Nature* 437: 249–252.

Faul U and Jackson I (2005) The seismological signature of temperature and grain size variations in the upper mantle. *Earth and Planetary Science Letters* 234: 119–234.

Fischer KM, Ford HA, Abt DL, and Rychert CA (2010) The lithosphere–asthenosphere boundary. *Annual Review of Earth and Planetary Sciences* 38: 551–575.

Fleitiout L and Yuen DA (1984) Secondary convection and the growth of the oceanic lithosphere. *Physics of the Earth and Planetary Interiors* 36: 181–212.

Fleitout L and Moriceau C (1992) Short-wavelength geoid, bathymetry and convective pattern beneath the Pacific Ocean. *Geophysical Journal International* 110: 6–28.

Forsyth DW (1992) Geophysical constraints on mantle flow and melt generation beneath mid-ocean ridges. In: Morgan P, Blackman DN, and Sinton M (eds.) *Evolution of Mid Ocean Ridges*. *Geophysical Monograph Series*, vol. 71, pp. 1–66. Washington, DC: American Geophysical Union.

Forsyth DW and The MELT Seismic Team (1998) Imaging the deep seismic structure beneath a mid-ocean ridge: The MELT experiment. *Science* 280: 1215–1218.

Frank FC (1968) Two component model for convection in the Earth's upper mantle. *Nature* 220: 350–352.

Freedman AP and Parsons B (1990) Geoid anomalies over two South Atlantic fracture zones. *Earth and Planetary Science Letters* 100: 18–41.

Gaboret C, Forte AM, and Montagner JP (2003) The unique dynamics of the Pacific Hemisphere mantle and its signature on seismic anisotropy. *Earth and Planetary Science Letters* 208: 219–233.

Gaherty JB, Jordan TH, and Lee LS (1996) Seismic structure of the upper mantle in a central Pacific corridor. *Journal of Geophysical Research* 101: 22291–22309.

Gaherty JB, Kato M, and Jordan TH (1999) Seismological structure of the upper mantle: A regional comparison of seismic layering. *Physics of the Earth and Planetary Interiors* 110(1–2): 21–41. http://dx.doi.org/10.1016/S0031-9201(98)00132-0.

Gans KD, Wilson DS, and Macdonald KC (2003) Pacific Plate gravity lineaments: Diffuse extension or thermal contraction? *Geochemistry, Geophysics, Geosystems* 4(9): 1074. http://dx.doi.org/10.1029/2002GC000465.

Goodwillie AM and Parsons B (1992) Placing bounds on lithospheric deformation in the central Pacific Ocean. *Earth and Planetary Science Letters* 111: 123–139.

Gribb TT and Cooper RF (1998) Low-frequency shear wave attenuation in polycrystalline olivine: Grain boundary diffusion and the physical significance of the Andrade model for viscoelastic rheology. *Journal of Geophysical Research* 103: 27267–27279.

Harmon N, Forsyth DW, and Scheirer DS (2006) Analysis of gravity and topography in the GLIMPSE study region: Isostatic compensation and uplift of the Sojourn and Hotu Matua Ridge systems. *Journal of Geophysical Research* 111: B11406. http://dx.doi.org/10.1029/2005JB004071.

Harmon N, Forsyth DW, Weeraratne DS, Yang Y, and Webb SC (2011) Mantle heterogeneity and off axis volcanism on young Pacific lithosphere. *Earth and Planetary Science Letters* 311(3): 306–315.

Haxby WF and Turcotte DL (1978) Isostatic geoid anomalies. *Journal of Geophysical Research* 83: 5473–5478.

Haxby WF and Weissel JK (1986) Evidence for small scale convection for SEASAT altimeter data. *Journal of Geophysical Research* 91: 3507–3520.

Hayes DE (1988) Age-depth relationships and depth anomalies in the Southeast Indian Ocean and South Atlantic Ocean. *Journal of Geophysical Research* 93: 2937–2954.
Heestand RL and Crough ST (1981) The effect of hot spots on the oceanic age–depth relation. *Journal of Geophysical Research* 86: 6107–6114.
Hernlund JW and Tackley PJ (2003) Post-Laramide volcanism and upper mantle dynamics in the western US: Role of small-scale convection. *EOS, Transactions, American Geophysical Union* 84(46), Fall Meet. Suppl., Abstract V31F-07.
Hirth G, Evans RL, and Chave AD (2000) Comparison of continental and oceanic mantle electrical conductivity: Is the Archean lithosphere dry? *Geochemistry, Geophysics, Geosystems* 1. http://dx.doi.org/10.1029/2000GC000048.
Hirth G and Kohlstedt DL (1996) Water in the oceanic upper mantle: Implications for rheology, melt extraction, and the evolution of the lithosphere. *Earth and Planetary Science Letters* 144: 93–108.
Huang J and Zhong S (2005) Sublithospheric small-scale convection and its implications for the residual topography at old ocean basins and the plate model. *Journal of Geophysical Research* 110: B05404. http://dx.doi.org/10.1029/2004JB003153.
Huang J, Zhong S, and van Hunen J (2003) Controls on sublithospheric small-scale convection. *Journal of Geophysical Research* 108: 2405. http://dx.doi.org/10.1029/2003JB002456.
Jackson I and Faul UH (2010) Grainsize-sensitive viscoelastic relaxation in olivine: Towards a robust laboratory-based model for seismological application. *Physics of the Earth and Planetary Interiors* 183: 151–163.
Jackson I, Fitz Gerald JD, Faul UH, and Tan BH (2002) Grain-size sensitive seismic-wave attenuation in polycrystalline olivine. *Journal of Geophysical Research* 107. http://dx.doi.org/10.1029/2002JB001225.
Jha K, Parmentier EM, and Sparks DW (1997) Buoyant mantle upwelling and crustal production at oceanic spreading centers: On-axis segmentation and off-axis melting. *Journal of Geophysical Research* 102: 11979–11989.
Johnson HP and Carlson RL (1992) Variation of sea floor depth with age: A test of model based on drilling results. *Geophysical Research Letters* 19: 1971–1974.
Kaminski É and Ribe NM (2001) A kinematic model for recrystallization and texture development in olivine polycrystals. *Earth and Planetary Science Letters* 189: 253–267.
Kaminski É and Ribe NM (2002) Timescales for the evolution of seismic anisotropy in mantle flow. *Geochemistry, Geophysics, Geosystems* 3: 1–17. http://dx.doi.org/10.1029/2001GC000222.
Karato S (1986) Does partial melting reduce the creep strength of the upper mantle. *Nature* 319: 309–310.
Karato S (2012) On the origin of the asthenosphere. *Earth and Planetary Science Letters* 321–322: 95–103. http://dx.doi.org/10.1016/j.epsl.2012.01.001.
Katz RF (2010) Porosity-driven convection and asymmetry beneath mid-ocean ridges. *Geochemistry, Geophysics, Geosystems* 11: Q0AC07. http://dx.doi.org/10.1029/2010GC003282.
Katzman R, Zhao L, and Jordan TH (1998) High-resolution, two-dimensional vertical tomography of the central Pacific mantle using ScS reverberations and frequency-dependent travel times. *Journal of Geophysical Research* 103: 17933–17972. http://dx.doi.org/10.1029/98JB00504.
Kawakatsu H, et al. (2009) Seismic evidence for sharp lithosphere–asthenosphere boundaries of oceanic plates. *Science* 324: 499–502.
Kelemen PB, Hirth G, Shimizu N, Spiegelman M, and Dick HJB (1997) A review of melt migration processes in the adiabatically upwelling mantle beneath oceanic spreading ridges. *Philosophical Transactions of the Royal Society A* 355: 282–318.
King SD and Anderson DL (1998) Edge-driven convection. *Earth and Planetary Science Letters* 160: 289–296.
Koppers AAP, Staudigel H, Pringle MS, and Wijbrans JR (2003) Short-lived and discontinuous intraplate volcanism in the South Pacific: Hot spots or extensional volcanism? *Geochemistry, Geophysics, Geosystems* 4: 1089. http://dx.doi.org/10.1029/2003GC000533.
Korenaga J (2007) Effective thermal expansivity of Maxwellian oceanic lithosphere. *Earth and Planetary Science Letters* 257: 343–349.
Korenaga J and Jordan TH (2002a) On 'steady-state' heat flow and the rheology of oceanic mantle. *Geophysical Research Letters* 29: 2056. http://dx.doi.org/10.1029/2002GL016085.
Korenaga J and Jordan TH (2002b) Onset of convection with temperature- and depth-dependent viscosity. *Geophysical Research Letters* 29(19): 1923. http://dx.doi.org/10.1029/2002GL015672.
Korenaga J and Jordan TH (2003a) Physics of multiscale convection in Earth's mantle: Onset of sublithospheric convection. *Journal of Geophysical Research* 108(B7): 2333. http://dx.doi.org/10.1029/2002JB001760.
Korenaga J and Jordan TH (2003b) Linear stability analysis of Richter rolls. *Geophysical Research Letters* 30(22): 2157. http://dx.doi.org/10.1029/2003GL018337.
Korenaga J and Jordan TH (2004) Physics of multiscale convection in Earth's mantle: Evolution of sublithospheric convection. *Journal of Geophysical Research* 109: B01405. http://dx.doi.org/10.1029/2003JB002464.
Korenaga T and Korenaga J (2008) Subsidence of normal oceanic lithosphere, apparent thermal expansivity, and seafloor flattening. *Earth and Planetary Science Letters* 268(1–2): 41–51. http://dx.doi.org/10.1016/j.epsl.2007.12.022.
Kumar P and Kawakatsu H (2011) Imaging the seismic lithosphere–asthenosphere boundary of the oceanic plate. *Geochemistry, Geophysics, Geosystems* 12: Q01006. http://dx.doi.org/10.1029/2010GC003358.
Langseth MG, LePichon X, and Ewing M (1966) Crustal structure of mid-ocean ridges. 5. Heat flow through the Atlantic Ocean and convection currents. *Journal of Geophysical Research* 71: 5321–5355.
Larson RL (1991) The latest pulse of the Earth – Evidence for a mid-Cretaceous superplume. *Geology* 19: 547–550.
Larson RL and Erba E (1999) Onset of mid-Cretaceous greenhouse in the Barremian–Aptian: Igneous events and the biological, sedimentary and geochemical responses. *Paleoceanography* 14: 663–678.
Lawrence JF and Shearer PM (2006) A global study of transition zone thickness using receiver functions. *Journal of Geophysical Research* 111: B06307. http://dx.doi.org/10.1029/2005JB003973.
Lekic V and Romanowicz B (2011) Inferring upper-mantle structure by full waveform tomography with the spectral element method. *Geophysical Journal International* 185(2): 799–831. http://dx.doi.org/10.1111/j.1365-246X.2011.04969.x.
Levitt DA and Sandwell DT (1995) Lithospheric bending at subduction zones based on depth soundings and satellite gravity. *Journal of Geophysical Research* 100: 379–400.
Li XQ, et al. (2004) Rejuvenation of the lithosphere by the Hawaiian plume. *Nature* 427(6977): 827–829. http://dx.doi.org/10.1038/nature02349.
Lin J and Parmentier EM (1985) Surface topography due to convection in a variable viscosity fluid: Application to short wavelength gravity anomalies in the central Pacific Ocean. *Geophysical Research Letters* 12: 357–360.
Lister CRB, Sclater JG, Davis EE, Villinger H, and Nagihara S (1990) Heat flow maintained in ocean basins of great age: Investigations in the north-equatorial west Pacific. *Geophysical Journal International* 102: 603–630.
Lizarralde D, Chave A, Hirth G, and Schultz A (1995) Northeastern Pacific mantle conductivity profile from long-period magnetotelluric sounding using Hawaii-to-California submarine cable data. *Journal of Geophysical Research* 100: 17837–17854.
Lundstrom CC (2003) Uranium-series disequilibria in mid-ocean ridge basalts: Observations and models of basalt genesis. In: Bourdon B, Henderson GM, Lundstrom CC, and Turner SP (eds.) *Uranium-Series Geochemistry*. *Reviews in Mineralogy and Geochemistry*, vol. 52, pp. 175–214. Washington, DC: Mineralogical Society of America.
Lynch MA (1999) Linear ridge groups: Evidence for tensional cracking in the Pacific Plate. *Journal of Geophysical Research* 104: 29321–29333.
Maggi A, Debayle E, Priestly K, and Barruol G (2006a) Multimode surface waveform tomography of the Pacific Ocean: A close look at the lithospheric cooling signature. *Geophysical Journal International* 166: 1384–1397.
Maggi A, et al. (2006b) Multimode surface waveform tomography of the Pacific Ocean: A closer look at the lithospheric cooling signature. *Geophysical Journal International* 166(3): 1384–1397. http://dx.doi.org/10.1111/j.1365-246X.2006.03037.x.
Maggi A, et al. (2006c) Azimuthal anisotropy of the Pacific region. *Earth and Planetary Science Letters* 250: 53–71. http://dx.doi.org/10.1016/j.epsl.2006.07.010.
Marquart G, Schmelling H, and Braun A (1999) Small-scale instabilities below the cooling oceanic lithosphere. *Geophysical Journal International* 138: 655–666.
Marty JC and Casanave A (1989) Regional variations in subsidence rate of oceanic plates: A global analysis. *Earth and Planetary Science Letters* 94: 301–315.
Marty J and Cazenave CA (1988) Thermal evolution of the lithosphere beneath fracture zones inferred from geoid anomalies. *Geophysical Research Letters* 15: 593–596.
Marty J, Cazenave CA, and Lago B (1988) Geoid anomalies across Pacific fracture zones. *Geophysical Journal* 93: 1–23.
McKenzie DP (1967) Some remarks on heat flow and gravity anomalies. *Journal of Geophysical Research* 72: 6261–6273.
McKenzie DP and Sclater JG (1969) Heat flow in the eastern Pacific and sea-floor spreading. *Bulletin of Volcanology* 33: 101–118.
McNutt MK (1998) Superswells. *Reviews of Geophysics* 36: 211–244.
Montagner J-P and Tanimoto T (1991) Global upper mantle tomography of seismic wave velocities and anisotropies. *Journal of Geophysical Research* 96: 20337–20351.
Morgan WJ (1968) Rises, trenches, great faults, and crustal blocks. *Journal of Geophysical Research* 73: 1959.

Morgan WJ (1971) Convection plumes in the lower mantle. *Nature* 230: 42–43.
Morgan WJ (1972) Deep mantle convection plumes and plate motions. *American Association of Petroleum Geologists Bulletin* 56: 203–213.
Nagihara S, Lister CRB, and Sclater JG (1996) Reheating of old oceanic lithosphere: Deductions from observations. *Earth and Planetary Science Letters* 139: 91–104.
Nettles M and Dziewonski AM (2008) Radially anisotropic shear velocity structure of the upper mantle globally and beneath North America. *Journal of Geophysical Research* 113: B02303. http://dx.doi.org/10.1029/2006JB004819.
Nishimura CE and Forsyth DW (1989) The anisotropic structure of the upper mantle in the Pacific. *Geophysical Journal* 96: 203–229.
O'Hara MJ (1965) Primary magmas and the origin of basalts. *Scottish Journal of Geology* 1: 19–40.
Oikawa M, Kaneda K, and Nishizawa A (2010) Seismic structures of the 154–160 Ma oceanic crust and upper mantle in the Northwest Pacific Basin. *Earth, Planets and Space* 62: e13–e16.
Okal EA and Batiza R (1987) Hotspots: The first 25 years. In: Keating BH, Fryer P, Batiza R, and Boehlert GW (eds.) *Seamounts, Islands, and Atolls*. *Geophysical Monograph*, vol. 43, pp. 1–11. Washington, DC: AGU.
Parmentier EM and Haxby WF (1986) Thermal stresses in the oceanic lithosphere: Evidence from geoid anomalies at fracture zones. *Journal of Geophysical Research* 91: 7193–7204.
Parmentier EM and Phipps Morgan J (1990) The spreading rate dependence of three-dimensional oceanic spreading center structure. *Nature* 348: 325–328.
Parsons B and McKenzie D (1978) Mantle convection and the thermal structure of the plates. *Journal of Geophysical Research* 83: 4485–4496.
Parsons B and Sclater JG (1977) An analysis of the variation of ocean floor bathymetry and heat flow with age. *Journal of Geophysical Research* 82: 803–827.
Passey QR (1981) Upper mantle viscosity derived from the difference in rebound of the Provo and Bonneville shorelines: Lake Bonneville Basin, Utah. *Journal of Geophysical Research* 86: 11701–11708.
Phipps Morgan J (1987) Melt migration beneath mid-ocean spreading centers. *Geophysical Research Letters* 14: 1238–1241.
Phipps Morgan J (1997) The generation of a compositional lithosphere by mid-ocean ridge melting and its effect on subsequent off-axis hotspot upwelling and melting. *Earth and Planetary Science Letters* 146: 213–232.
Phipps Morgan J and Parmentier EM (1995) Crenulated seafloor: Evidence for spreading rate dependent structure of mantle upwelling and melting beneath a mid-oceanic spreading center. *Earth and Planetary Science Letters* 129: 73–84.
Priestley D and McKenzie DM (2006) The thermal structure of the lithosphere from shear velocities. *Earth and Planetary Science Letters* 244: 285–301.
Rabinowicz M and Ceuleneer G (2005) The effect of sloped isotherms on melt flow in the shallow mantle: A physical and numerical model based on observations in the Oman ophiolite. *Earth and Planetary Science Letters* 229: 231–246.
Raddick MJ, Parmentier EM, and Scheirer DS (2002) Buoyant decompression melting: A possible mechanism for intraplate volcanism. *Journal of Geophysical Research* 107(B10): 2228. http://dx.doi.org/10.1029/2001JB000617.
Renkin ML and Sclater JG (1988) Depth and age in the North Pacific. *Journal of Geophysical Research* 93: 2910–2935.
Richards MA, Duncan RA, and Courtillot VE (1989) Flood basalts and hot-spot tracks: Plume heads and tails. *Science* 246: 103–107.
Richter FM (1973) Convection and the large scale circulation of the mantle. *Journal of Geophysical Research* 74: 8735–8745.
Richter FM and Parsons B (1975) On the interaction of two scales of convection in the mantle. *Journal of Geophysical Research* 80: 2529–2541.
Ritzwoller MH, Shapiro NM, and Zhong SJ (2004) Cooling history of the Pacific lithosphere. *Earth and Planetary Science Letters* 226(1–2): 69–84. http://dx.doi.org/10.1016/j.epsl.2004.07.032.
Rychert CA, Schmerr N, and Harmon N (2012) The Pacific lithosphere–asthenosphere boundary: Seismic imaging and anisotropic constraints from SS waveforms. *Geochemistry, Geophysics, Geosystems* 13: Q0AK10. http://dx.doi.org/10.1029/2012GC004194.
Rychert CA and Shearer PM (2011) Imaging the lithosphere–asthenosphere boundary beneath the Pacific using SS waveform modeling. *Journal of Geophysical Research* 116: B07307. http://dx.doi.org/10.1029/2010JB008070.
Sandwell DT (1984) Thermomechanical evolution of oceanic fracture zones. *Journal of Geophysical Research* 89: 11401–11413.
Sandwell D and Fialko Y (2004) Warping and cracking of the Pacific plate by thermal contraction. *Journal of Geophysical Research* 109: B10411. http://dx.doi.org/10.1029/2004JB003091.
Sandwell DT and McAdoo DC (1988) Marine gravity of the southern ocean and Antarctic margin from Geosat. *Journal of Geophysical Research* 93: 10389–10396.
Sandwell D and Schubert G (1980) Geoid height versus age for symmetric spreading ridges. *Journal of Geophysical Research* 85: 7235–7241.
Sandwell DT and Schubert G (1982a) Geoid height-age relation from SEASAT altimeter profiles across the Mendocino fracture zone. *Journal of Geophysical Research* 87: 3949–3958.
Sandwell DT and Schubert G (1982b) Lithospheric flexure at fracture zones. *Journal of Geophysical Research* 87: 4657–4667.
Sandwell DT and Smith WHF (1997) Marine gravity anomaly from Geosat and ERS 1 satellite altimetry. *Journal of Geophysical Research* 102: 10039–10054. http://dx.doi.org/10.1029/96JB03223.
Sandwell DT, Winterer EL, Mammerickx J, et al. (1995) Evidence for diffuse extension of the Pacific plate from Pukapuka Ridges and Cross-Grain gravity lineations. *Journal of Geophysical Research* 100: 15087–15099.
Schlanger SO, Garcia MO, Keating BH, et al. (1984) Geology and geochronology of the Line Islands. *Journal of Geophysical Research* 89: 11261–11272.
Schmerr N (2012) The Gutenberg discontinuity: Melt at the lithosphere–asthenosphere boundary. *Science* 335(6075): 1480–1483. http://dx.doi.org/10.1126/science.1215433.
Schroeder W (1984) The empirical age–depth relation and depth anomalies in the Pacific Ocean. *Journal of Geophysical Research* 89: 9873–9884.
Schubert G, Froidevaux C, and Yuen DA (1976) Oceanic lithosphere and asthenosphere: Thermal and mechanical structure. *Journal of Geophysical Research* 81: 3525–3540.
Schubert G and Turcotte DL (1972) One dimensional model of shallow mantle convection. *Journal of Geophysical Research* 77: 945–951.
Schubert G, Yuen DA, Froidevaux C, Fleitout L, and Souriau M (1978) Mantle circulation with partial shallow return flow. *Journal of Geophysical Research* 83: 745–758.
Sclater JG, Lawver LA, and Parsons B (1975) Comparison of long-wavelength residual elevation and free air gravity anomalies in the north Atlantic and possible implications for thickness of the lithospheric plate. *Journal of Geophysical Research* 80: 1031–1052.
Sigmundsson F (1991) Post-glacial rebound and asthenosphere viscosity in Iceland. *Geophysical Research Letters* 18: 1131–1134. http://dx.doi.org/10.1029/91GL01342.
Sleep NH (1969) Sensitivity of heat flow and gravity to the mechanism of seafloor spreading. *Journal of Geophysical Research* 74: 542–549.
Smith WHF (1998) Seafloor tectonic fabric from satellite altimetry. *Annual Review of Earth and Planetary Sciences* 26: 697–738.
Sparks DW and Parmentier EM (1991) Melt extraction from the mantle beneath spreading centers. *Earth and Planetary Science Letters* 105: 368–377.
Sparks DW and Parmentier EM (1993) The structure of three-dimensional convection beneath spreading centers. *Geophysical Journal International* 112: 81–91.
Spiegelman M (1993) Physics of melt extraction: Theory, implications and applications. *Philosophical Transactions of the Royal Society A* 342: 23–41.
Spiegelman M and Elliot T (1993) Consequences of melt transport for Uranium series disequilibrium. *Earth and Planetary Science Letters* 118: 1–20.
Spiegelman M and Kelemen PB (2003) Extreme chemical variability as a consequence of channelized melt transport. *Geochemistry, Geophysics, Geosystems* 4(7): 1055. http://dx.doi.org/10.1029/2002GC000336.
Spiegelman M and McKenzie D (1987) Simple 2-D models for melt extraction at mid-ocean ridges and island arcs. *Earth and Planetary Science Letters* 83: 137–152.
Stein CA and Stein S (1992) A model for the global variation in oceanic depth and heat flow with lithospheric age. *Nature* 359: 123–129.
Stein CA and Stein S (1993) Constraints on Pacific midplate swells from global depth-age and heat flow-age models. In: Pringle MS, et al. (eds.) *The Mesozoic Pacific: Geology, Tectonics, and Volcanism*. *Geophysical Monograph Series*, vol. 77, pp. 53–76. Washington, DC: AGU.
Stixrude L and Lithgow-Bertelloni C (2005) Mineralogy and elasticity of the oceanic upper mantle: Origin of the low-velocity zone. *Journal of Geophysical Research* 110: B03204. http://dx.doi.org/10.1029/2004JB002965.
Stolper E (1980) A phase diagram for mid-ocean ridge basalts: Preliminary results and implications for petrogenesis. *Contributions to Mineralogy and Petrology* 74: 13–27.
Sundberg M and Cooper RF (2010) A composite viscoelastic model for incorporating grain boundary sliding and transient diffusion creep: Correlating creep and attenuation responses for materials with a fine grain size. *Philosophical Magazine* 90: 2817–2840.
Tackley PJ and Stevenson DJ (1993) A mechanism for spontaneous self-perpetuating volcanism on the terrestrial planets. In: Stone DB and Runcorn SK (eds.) *Flow and Creep in the Solar System: Observations, Modeling and Theory*, pp. 307–321. Norwell, MA: Kluwer Academic.
Tan Y and Helmberger DV (2007) Trans-Pacific upper mantle shear velocity structure. *Journal of Geophysical Research* 112: B08301. http://dx.doi.org/10.1029/2006JB004853.

Turcotte DL and Oxburgh ER (1967) Finite amplitude convective cells and continental drift. *Journal of Fluid Mechanics* 28: 24–42.

Turner DL and Jarrard RD (1982) K–Ar dating of the Cook–Austral island chain: A test of the hot-spot hypothesis. *Journal of Volcanology and Geothermal Research* 12: 187–220.

van Hunen J, Huang J, and Zhong S (2003) The effect of shearing on the onset and vigor of small-scale convection in a Newtonian rheology. *Geophysical Research Letters* 30(19): 1991. http://dx.doi.org/10.1029/2003GL018101.

Vogt PR and Ostenso NA (1967) Steady state crustal spreading. *Nature* 215: 811–817.

Wang D, Mookerjee M, Xu Y, and Karato S (2006) The effect of water on the electrical conductivity of olivine. *Nature* 443: 977–980. http://dx.doi.org/10.1038/nature05256.

Weeraratne DS, Forsyth DW, Yang Y, and Webb SC (2007) Rayleigh wave tomography beneath intraplate volcanic ridges in the South Pacific. *Journal of Geophysical Research* 112(B6): B06303.

Wenk H-R and Tomé CN (1999) Modeling dynamic recrystallization of olivine aggregates deformed in simple shear. *Journal of Geophysical Research* 104: 25513–25528. http://dx.doi.org/10.1029/1999JB900261.

Wessel P (2001) Global distribution of seamounts inferred from gridded Geosat/ERS-1 altimetry. *Journal of Geophysical Research* 106: 19431–19441.

Wessel P and Haxby WF (1990) Thermal-stresses, differential subsidence, and flexure at oceanic fracture zones. *Journal of Geophysical Research* 95: 375–391.

Wessel P, Kroenke LW, and Bercovici D (1996) Pacific Plate motion and undulations in geoid and bathymetry. *Earth and Planetary Science Letters* 140: 53–66.

Wessel P and Lyons S (1997) Distribution of large Pacific seamounts from Geosat/ERS-1: Implications for the history of intraplate volcanism. *Journal of Geophysical Research* 102: 22459–22475.

Yoshino T, Matsuzaki T, Yamashita S, and Katsura T (2006) Hydrous olivine unable to account for conductivity anomaly at the top of the asthenosphere. *Nature* 443: 973–976. http://dx.doi.org/10.1038/nature05223.

Yuen DA and Fleitout L (1984) Stability of the oceanic lithosphere with variable viscosity: An initial-value approach. *Physics of the Earth and Planetary Interiors* 343: 173–185.

Zaranek SE and Parmentier EM (2004) Convective instability of a fluid with temperature-dependent viscosity cooled from above. *Earth and Planetary Science Letters* 224: 371–386.

Zhou Y, Nolet G, Dahlen FA, and Laske G (2006) Global upper-mantle structure from finite-frequency surface-wave tomography. *Journal of Geophysical Research* 111: B04304. http://dx.doi.org/10.1029/2005JB003677.